The Spatial Distribution Assessment of Particulate Matter by Biomagnetic Monitoring Using *Phoenix dactylifera* Leaf Samples and Azimuthal Dust Samplers in Kuwait

Athari Almutawa[1,2], Samson Roeland[1]

[1]Laboratory of Environmental and Urban Ecology, Department of Bioscience Engineering, University of Antwerp, Antwerpen, Belgium
[2]Department of Desert Rehabilitation and Restoration, Public Authority of Agriculture and Fisheries, Rabia, Safat, Kuwait
Email: Almutawa.Athari@uantwerpen.be, roeland.samson@uantwerpen.be

Abstract

This study employs multi-magnetic parametric methods as proxies to measure particulate matter (PM) concentration and spread in Kuwait. It examines the reliability of biomonitoring receptors in the assessment of atmospheric air quality through the utilization of passive biomonitoring methodology using cleaned and non-cleaned *Phoenix dactylifera* leaves and active biomonitoring through the application of dust samplers in the study area. Four radial sampling areas are located at 2, 6, 10, 14 km from Kuwait's city center with 10 sampling degree points selected from each radial area, and the closest palm tree in the vicinity to the preselected sampling point with a height of 4 m were sampled. Using a compass, the 4 azithumal points were pin pointed on the selected tree and a 2 × 2 cm dust sampler was attached to each direction at a height of 2 m. The dust sampler was made of clear plastic paper attached with double sided tape. Magnetic susceptibility and Saturation Isothermic Remanent Magnetization (SIRM), Natural Remanent Magnetization (NRM), Hard Isothermal Remanent Magnetization (HIRM), Soft Isothermal Remanent Magnetization (SOFT), HIRM%, soft IRM% and *s*-ratio were determined for *P. dactylifera* and dust samplers. Magnetic parameters were mapped to assess the spatial variation of air quality in Kuwait and the values between dust samplers and *P. dactylifera*. Results indicate that the highest magnetic concentration values for NRM and SIRM for *P. dactylifera* occurred near Kuwait bay and that the majority of the samples contain ferromagnetic minerals with magnetite most likely from anthropogenic sources. The results of the interpolation

models for *P. dactylifera* and dust samplers as well as the overall mean for dust samplers distinguished short-term PM deposition and concentration and how it is impacted by wind direction in comparison to *P. dactylifera* which identifies long-term pollution impacts pin pointing PM sources and hotspots.

Keywords

Kuwait, Magnetic, Spatial Distribution, Azithumal Degree, Wind Direction, Biomonitor

1. Introduction

Particulate matter (PM) is a detrimental threat to the environment and the health of residents in urban areas. It is associated with a variety of respiratory and cardiovascular diseases such as: asthma, lung cancer, heart attacks and respiratory infections [1] [2]. Ambient airborne particulate matter (PM) is defined by Chen *et al.* (2016) as airborne particles which are grouped as coarse, fine, and ultrafine particles (UFPs) with aerodynamic diameters within 2.5 to 10 μm (PM_{10}), and <2.5 μm ($PM_{2.5}$), and <0.1 μm ($PM_{0.1}$), respectively. High concentrations of PM are associated with industrial emissions, roadways, construction, road dust, traffic emissions and its concentrations are influenced by humidity, wind speed, direction and turbulence [3] [4] [5]. Wind events can mobilize and transport surficial soils over a range of distances depending on their mass, with large particles travelling at short distances and having a higher rate of sedimentation in comparison to small particles [6]. These airborne PM derived from surficial soils can be traced to its source or point of origin as it has a geochemical signature and contaminant loadings from the original source material [6].

The highest amounts of dust emissions are Australia, Arabia, China and Central Asia, and the Sahara regions [7]. The Arabian Peninsula generates approximately 11% of the global airborne mineral dust mass [8]. Therefore, environmental and health risks are higher in Kuwait especially as it is an arid, semi-arid region where uptake and erosion/leaching processes are less pronounced and frequent sand and dust storms are encountered [6]. The number of dusty days and daily PM10 concentration are rising further as a result of climate change, desertification, urbanization land use change and anthropogenic influences [6] [9] [10] [11]. Dust storms occur as a result of turbulent winds raising large quantities of dust from surfaces, that can reach up to 6000 μgm^{-3} in severe events [10] [12]. Aerosols, particulates and pollutants are easily transferred across the peninsula by dust storms, chemically made of SiO_2 (60%), Al_2O_3 (14%), Fe_2O_3 (7%), CaO (4%), MgO (2.6%) and K_2O (2.4%) and are mineralogically dominated by quartz, magnetite/hematite and carbonates [9] [13].

PM source appointment in Kuwait presents a challenge as it is a small country neighboring several countries that are also engaged in the petroleum and gas industry and chemical manufacturing that are possibly contributing sources of

pollution [14]. There are several studies that have tackled the topic of air quality in Kuwait covering; source appointment and mineralogical compositions of dust [14] [15]; PTE contamination and enrichment in soil [6], spatial and seasonal variations of the PM10 [16]; vegetation and soil conditions [17] and dust fallout [18] [19]. These traditional studies on characterization of suspended PM and assessment of air quality in Kuwait dust have been primarily based on geochemical and mineralogical methods, while magnetic properties of suspended dust have yet to be examined.

As well as the majority of pollution exposure data is often sourced from low partial-resolution networks of monitoring stations that are incapable of capturing fine scale variations in PM concentration and/or particle size across diverse urban environment at pedestrian exposure height [20]. The geochemical and magnetic properties of transported materials, and their inter-relationships may be affected due to changes in the composition of transported materials from near-surface wind fields hindering the identification of the source material [21].

The application of environmental magnetism as a proxy for atmospheric pollution levels enables the identification of magnetic components, the determination of PM transport, daily atmospheric PM concentration, relative contribution at a given site, atmospheric heavy metals provenance, their distribution and localization in addition to being proxy underlying environmental processes [22] [23] [24]. Biomonitoring of air quality through the utilization of plant leaves and bark has been proven to be more economical and time effective at larger and more diverse spatial scale set-ups, especially in unforeseen releases and accidental situations [25] [26]. Plants have the capacity to accumulate PM, they capture PM through dry and wet deposition onto leaf surface areas by gravity, diffusion and turbulent transfer giving rise to impaction and interception and root uptake [27] [28] [29]. Though, PM capture is affected by specific species characteristics such as: trichome density, leaf surface size, leaf hydrophobicity, chemical composition and structures of epicuticular waxes and plant height [30].

Two types of biomonitoring passive and active biomonitoring can be applied. Passive biomonitoring reflects more long-term changes in environmental quality, it has some limitations such as: the scale of a study can be restrained due to varying environmental conditions, local situations and survey area characteristics as well as the limitation of species variety or mass and their morphological and physiological differences in a given location [25] [26] [31]. However, active biomonitoring overcomes these limitations as selected species or sampling equipment can be translocated to the study area for a specified duration of time enabling the use of the same species on a larger scale, independently of its natural occurrence giving spatial and temporal information on sources and deposition patterns of atmospheric contaminants leading to a higher degree of standardization [25] [32].

There have been recommendations towards washing leaf surfaces prior to

biomonitoring studies to ensure particles of edaphic origin are detached and the standardization of samples from any environmental factors [33]. There are relatively few studies that compare passive and active biomonitoring studies of the same regions and these focus on the geochemical concentrations of air pollutants and utilize plants species and mosses that are not present in arid dry regions (e.g. Ştefănuţ *et al.* 2021, da Costa *et al.* 2016; Fleck *et al.* 2016) [25] [34] [35]. In this study, dust samplers will be applied as active biomonitors and *P. dactylifera as* passive biomonitors in the assessment of PM in a Kuwait by determining the relationship between street dust and airborne dust particles as passive dust characteristics are intermediate between street dust and airborne dust particles [7]. This study aims to: 1) assess if pre-treating leaf surfaces by cleaning them yields similar results to passive biomonitoring; 2) evaluate if magnetic parameters yield different responses for active and passive biomonitoring as indicators for PM loadings in the study area; 3) assess if azithumal direction at the same sampling point in passive biomonitoring affects PM concentration and mineralogy; 4) compare and evaluate if there is a relationship between magnetic properties and ambient PM spatial distribution for passive and active biomonitoring.

2. Material and Methods

2.1. Study Area

Kuwait is a small country covering an area of 17,818 km^2, located in the Middle East, bordering Iraq to the north and Saudi Arabia to the south and the Persian Gulf to the east. Kuwait's topography is gravelly and sandy desert with low to moderate relief, with more than 50 percent of Kuwait desert is covered by aeolian sand [17] [36]. The climate is characterized as hot, dry summers (May-September) with temperatures reaching up to 45˚C and mild winters (October-April), dropping to 8˚C [17]. It has a mean annual rainfall of 119 mm, while mean annual potential evapo-transpiration exceeds 2270 mm [18]. Sand and dust storms are frequent during the summer between March and August, they extend in a NW-SE direction, with dominant northwesterly winds forming 60% of the total wind directions and from the southeast at a lesser extent and shorter duration [36] [37]. The average monthly wind speed ranges in January and December are from 10 to 12.8 mph in June and July, with 12% of the year having a calm wind [4].

There are five major dust sources areas: the southwestern desert of Iraq; Mesopotamian flood plain in Iraq; north eastern desert of Saudi Arabia; drained marshes (Ahwar) area in southern Iraq; and Sabkhas, dry marshes and abandoned farms in Iran at the northern coastal area of the Arabian Gulf [19] [37]. Dust events that occur can affect air temperature through the transportation of aerosols and desert dust modifying radiation fields balance by cooling or heating surface temperatures and between atmospheric layers that can last for several hours depending on several factors like the surface albedo and dust layer eleva-

tion [9] [38]. Measurements were taken at 4 radial sampling areas (2, 6, 10, 14 km) from Kuwait's City center from 10 sampling points that were selected at (248, 238, 226, 216, 206, 196, 184, 174, 165, 154) degrees at each radial area, sampling 40 locations in total (Figure 1). Sampling occurred from the 26th January to the 8th February 2019. A wind rose indicating wind speed and direction for the sampling duration (Figure 2).

2.2. Biomonitoring

2.2.1. Passive Biomonitoring

The species sampled in this study is *P. dactylifera*, it was selected as it is widely used and distributed as an ornamental street tree or in parks in Kuwait. Tree species with a similar height of 4 m were selected, to ensure that they have similar exposure time. The tree nearest to the vicinity of the preselected sampling point with a height of 4 m was sampled. Sampled leaves were selected on the basis of having no abnormalities or not suffering from nutrient deficiencies as well as being of similar leaf or frond size. Leaves were collected every 70 azimuthal degrees from the lower one third of the canopy of each tree and were not wiped cleaned and referred to as *P. dactylifera* (NW). To tests if cleaned leaves had an
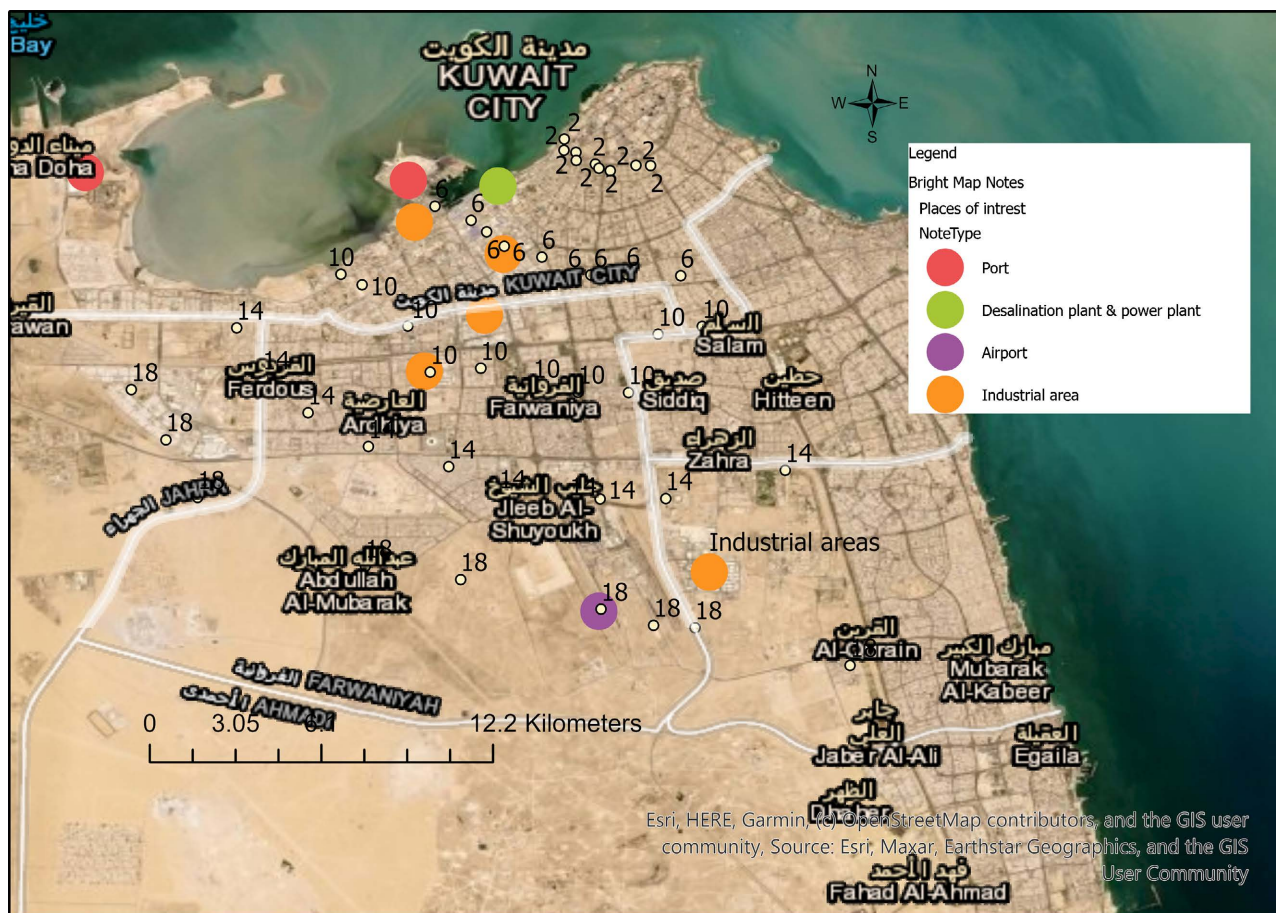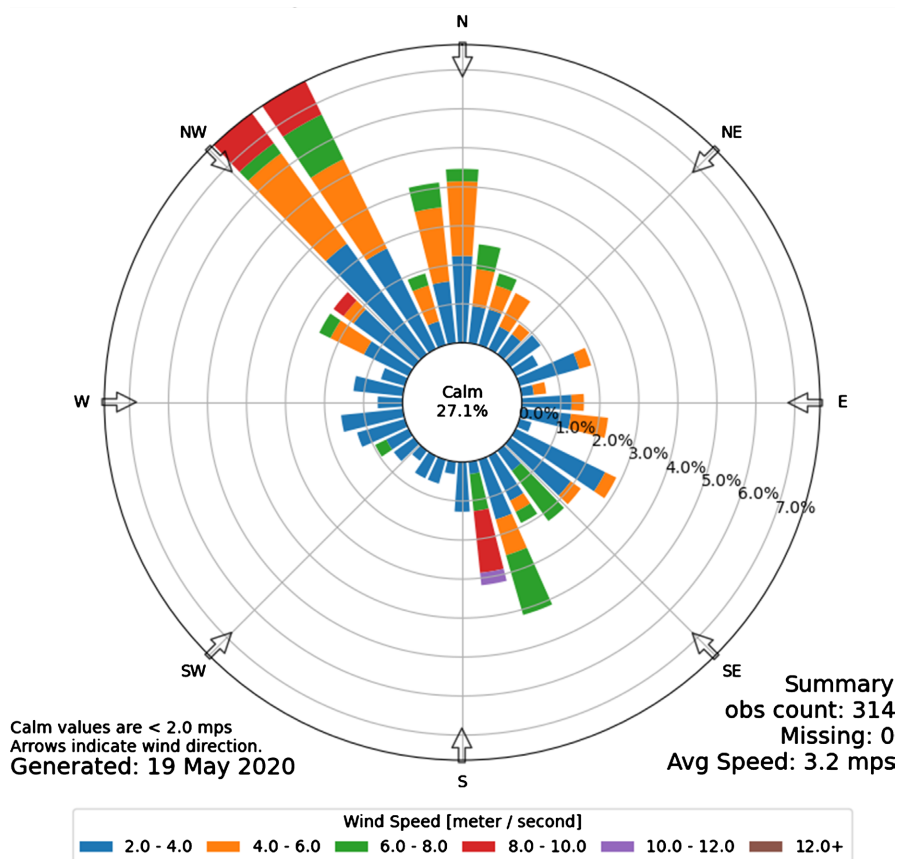

Figure 1. Map indicating sampled locations Kuwait by radial area (units: km) and decimal degrees (west to east) where sampling was conducted at (248, 236, 226, 216, 206, 196, 184, 174, 164, 154 degrees) moving away from Kuwait's city center.

Figure 2. Wind rose plot indicting mean wind direction and speed in Kuwait during sampling duration period: 26th January 2019 to 8th February (source: IEMS). Calm = indication of wind speeds below 2.0 m·s⁻¹.

effect on magnetic mineral accumulation rate, ten wiped *P. dactylifera* (W) samples at the radial distance of 2 km from Kuwait City, Kuwait's city center were selected. The leaf surfaces were cleaned with a wet wipe and marked with tape and then collected after a period of 2 weeks. On the day of the collection surface area of the leaf samples were measured by scanning the leaves and analyzed using a Java-based public domain image processing and analysis program, ImageJ which is developed at the National Institutes of Health (NIH), USA. Leaf samples were collected and stored in paper envelopes and transported to Public Authority of Agriculture and Fisheries, Kuwait (PAAF) and left to air dry for 4 days. Samples were then weighed and wrapped in an A4 cling wrap film and transported to the research lab at the Bioscience Engineering Department of the University of Antwerp, Belgium for analysis.

2.2.2. Active Biomonitoring

Dust was collected using a sampler that was made using a clear plastic paper, cut to an area of 4 × 2 cm, with a 2 × 2 double sided tape attached at the back, the extra 1 cm of plastic on the sampler is placed as to avoid physical contact and contamination of the dust sampler during the attachment and removal of the sample. Using a compass the 4 cardinal points (N, S, E and W) were pinpointed

at the trunk and the samplers were then attached around the trunk of the selected tree within the vicinity of the sampling point at a height of 2 m in order to test human exposure to the existing atmospheric pollution, using plastic tip push pins. Each sampler was labelled with the directions (N, S, E and W) to test the effect of wind direction on PM deposition. Dust samplers were attached for a duration of 2 weeks, during the collection of the samplers the extra 1cm of plastic that was on each side of the sampler without double sided tape that was placed to avoid sample contamination through handling was disposed of. Samples were collected and stored in paper envelopes and transported to Public Authority of Agriculture and Fisheries, Kuwait (PAAF). Each sample was then wrapped in an A4 cling wrap film and to the research lab at the Bioscience Engineering Department of the University of Antwerp, Belgium for analysis.

2.3. Magnetic Measurements

Magnetic measurements were conducted at the laboratory of the Departments of Bioscience Engineering of the University of Antwerp, Belgium. Dried leaf samples and dust samplers were first wrapped in A4 plastic cling wrap and placed in a 6.7 cm^3 plastic cube container. Initially the magnetic susceptibility of the samples was measured at room temperature using a Barrington MS2B magnetic susceptibility magnetometer (Barrington Ltd., U.K.). Samples were first tested for low frequency (χ_{LF}) and then high frequency (χ_H) enabling frequency dependent susceptibility χ_{FD} (%) to be calculated. However, χ_{FD} (%) could not be calculated for dust sampler as readings were too low for χ_{LF}.

Samples were then measured for natural remnant magnetization (NRM). Then individually magnetized in a direct current (DC) field of 1T and measured for saturated isothermal magnetization (SIRM). Followed by individually magnetized in a direct current (DC) field of 1T and measured for saturated isothermal magnetization and then magnetized at reverse fields −20 mT and −300 mT to measure SOFT (IRM$_{-20mT}$), HIRM (IRM$_{-300mT}$) (Equations (1)-(3)). All magnetizations were carried out using a Molespin pulse magnetizer (Molspin Ltd., UK) and followed by measurement using an AGICO magnetometer. SOFT and HIRM magnetic parameters were also converted to percentages (Equations (4) & (5)). The s-ratio was calculated to determine the relative concentration of antiferromagnetic material. Each sample was measured thrice to avoid measurement errors and values were normalized to a sampling pot volume of (10 cm^3) and by average specific leaf and sampler area (cm^2) to obtain a normalized value final SIRM value expressed as µA (A = A m^2/m^2).

$$\text{SOFT} = \left(\text{SIRM} - \text{IRM}_{-20}\right)/2 \tag{1}$$

$$\text{HIRM} = \left(\text{SIRM} - \text{IRM}_{-300}\right)/2 \tag{2}$$

$$\text{Soft IRM\%} = \text{SOFT}/\text{SIRM} \times 100 \tag{3}$$

$$\text{Hard IRM\%} = \text{HIRM}/\text{SIRM} \times 100 \tag{4}$$

$$s\text{-ratio} = \text{IRM}_{-300}/\text{SIRM} \tag{5}$$

2.4. Statistical Analysis

Statistical analysis was performed using Statistical Package for Social Science (SPSS, (21.0)). Descriptive statistics were calculated for NRM, SIRM, s-ratio, HIRM, SOFT, SOFT% and HIRM% for radial distance, sampling degree and azithumal direction. ANOVAs were performed to identify the possible effects of radial distance, sampling degree and azithumal direction on magnetic values NRM, SIRM, HIRM, SOFT, HIRM%, SOFT%. Pearson's correlation coefficients were performed to test the relationship.

A factorial analysis was carried out to identify whether there are any correlations between the various magnetic parameters. An exploratory factorial analysis was applied, because there is no a previous structure of factors to be tested. Extraction method of factors was conducted through unweighted least squares (ULS), because other approaches (maximum likelihood ML) did not reach convergence. The choice of the number of factors is based on the Kaiser's criteria (eigen values higher than 1). Varimax rotation was conducted in order to simplify relationships between factors and variables. The assigning of parameters to factors to carry out interpretations consists of saturation retentions > 0.5.

2.5. Spatial Distribution Mapping

The spatial variation of magnetic parameters and difference between azithumal directions for leaf and dust samplers were illustrated using geostatistical interpolation using Kriging, with a power of 2 to indicate the variance of magnetic concentration and grain size based on the distance on the direction and distance of two sampling locations, using ArcGIS (10.6.1) (Environmental System Research Institute (ESRI), Redlands, Canada). It models the trend as a linear function with independent external variables it derives the local mean (trend) of the dependent magnetic variables enabling the assessment of values at unobserved locations [39]. Kriging produces unbiased predictions with minimal variance based on the principle that variables are regionalized and utilizes the spatial structure of the data [40]. The overall mean of dust sampler of each magnetic parameter was inputted to compare passive biomonitoring techniques to active biomonitoring.

3. Results

3.1. Active and Passive Biomonitoring

P. dactylifera samples for (W) values were lower than (NW) values for NRM, SIRM and s-ratio. There was correlation between NRM and radius for *P. dactylifera* (p = 0.001). Overall radial distances there was a difference between mean s-ratio, SIRM and NRM for *P. dactylifera* (W) and *P. dactylifera* (NW) was 0.1, 22.58 μA and 2.24 μA. A multiple regression model was adjusted by radius, this exhibited that for two sample points in the same direction and radius, there were significant differences for NRM values between (W) and (NW) *P. dactylifera*

samples (p = 0.009). SIRM at the 2 km radial distance at every sampling point, was determined to be close to statistical significance for *P. dactylifera* (W) and (NW) (p = 0.064). *s*-ratio at the 2 km radial distance at every sampling point, was determined to be close to statistical significance for *P. dactylifera* (W) and (NW) (p = 0.039). The correlation between radial distance, sampling degree and HIRM was observed at the 2 km radial distance, between (W) and (NW) (p = 0.039).

For *P. dactylifera* (W) a contrary association was observed for HIRM (%) and radius (p = 0.017), with the beta coefficient being negative (−0.374). Radial distance affected NRM and HIRM, with NRM values dropping linearly as radial distance increased away from the city center, indicating a 90% difference between radial distances of 2 and 14 km, (p = 0.001). The contrary was perceived for HIRM values as they rose with distance by 34%, 52% and 9% at 6, 10, 14 km, respectively. While for dust samplers NRM values increased with increasing radial distance (p = 0.002). Figure 3 indicates that distance has the same impact on NRM and is independent of azithumal direction. The south azithumal direction is the lowest of the group (Figure 3), whereas, SIRM was the lowest at 10 km at 85.54 μA > 6 km at 124.96 μA > 2 km at 183.95 μA > 14 km at 190.57 μA. The average *s*-ratio for dust samplers for overall radial distances is 0.96, with *s*-ratio increasing as distance increases (p = 0.005). Overall NRM for dust samplers
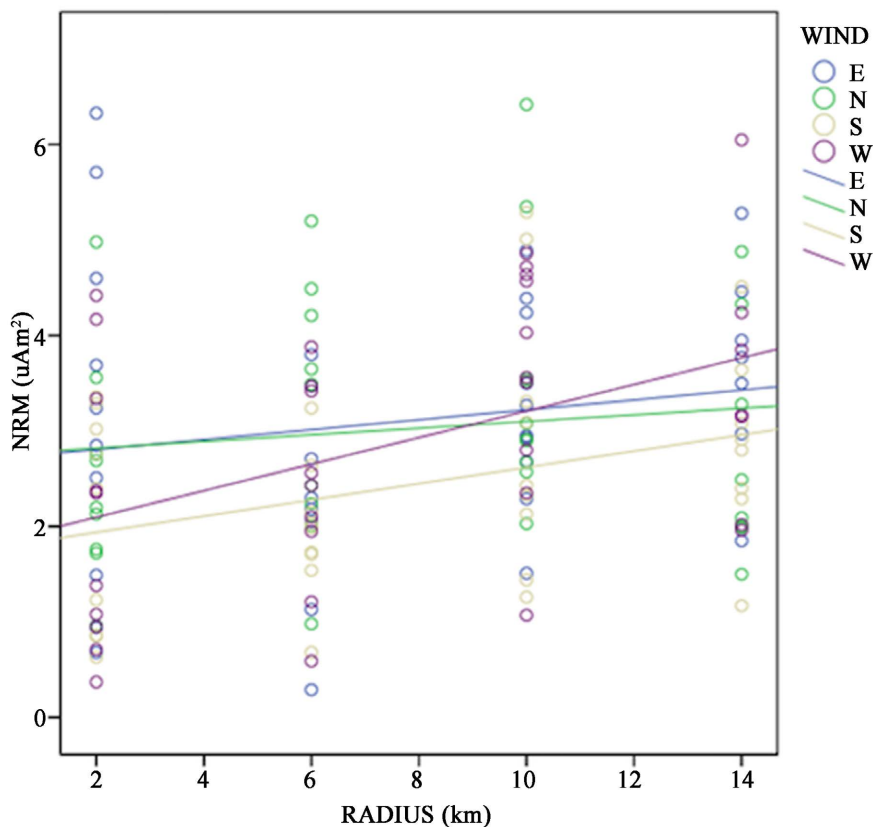
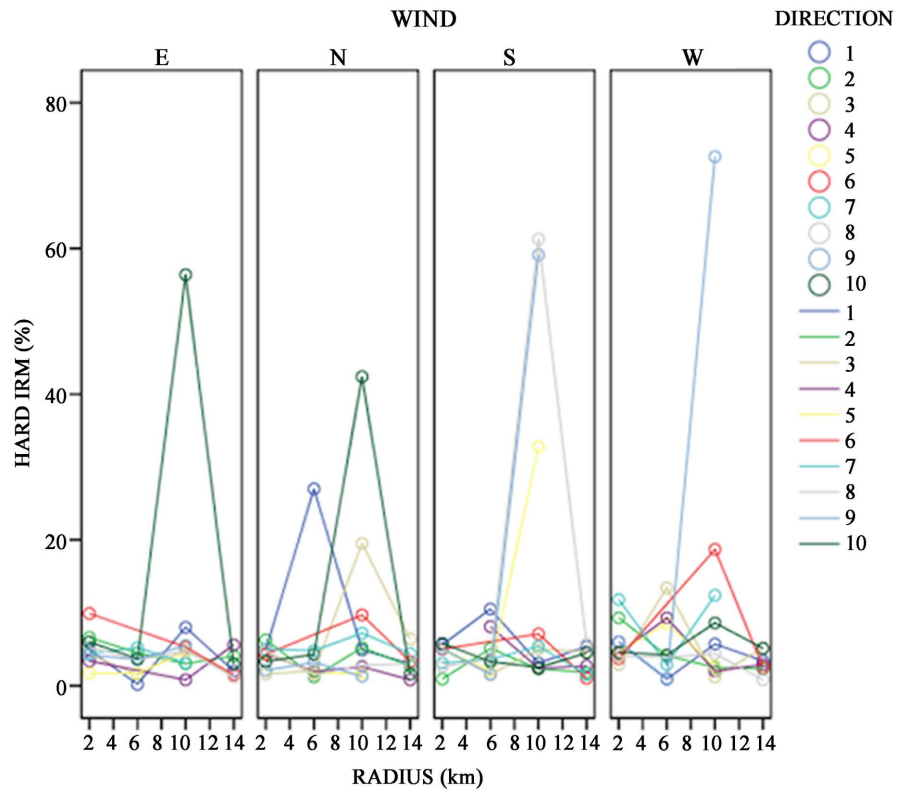**Figure 3.** NRM (μA) of dust sampler over radial distances (unit: 2, 6, 10, 14 km). Four regression lines show line of best fit.
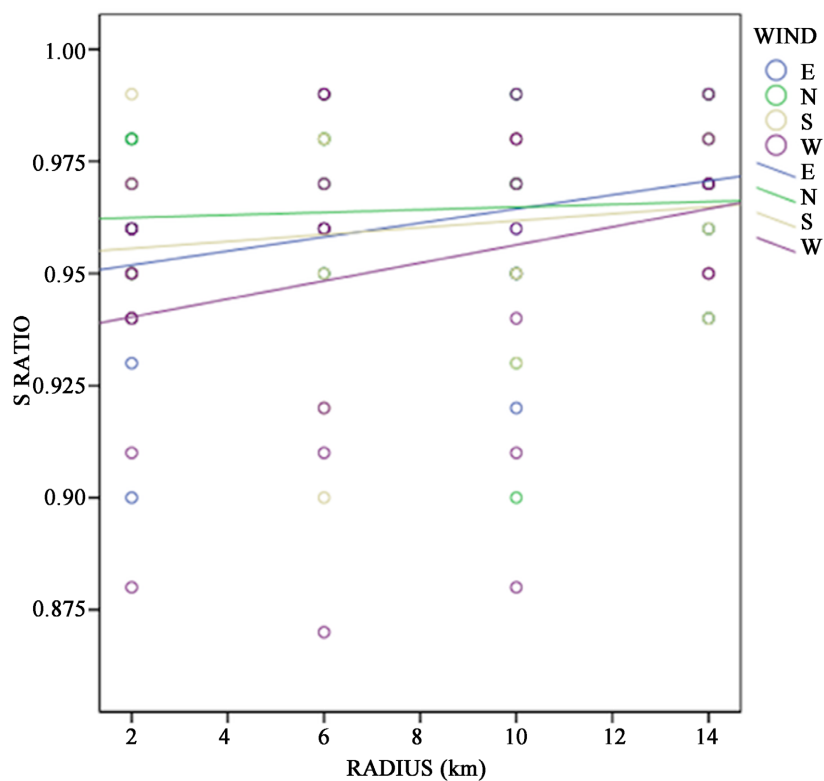
Figure 4. *s*-ratio (μA) of dust sampler over radial distances (unit: 2, 6, 10, 14 km). Four regression lines show line of best fit.
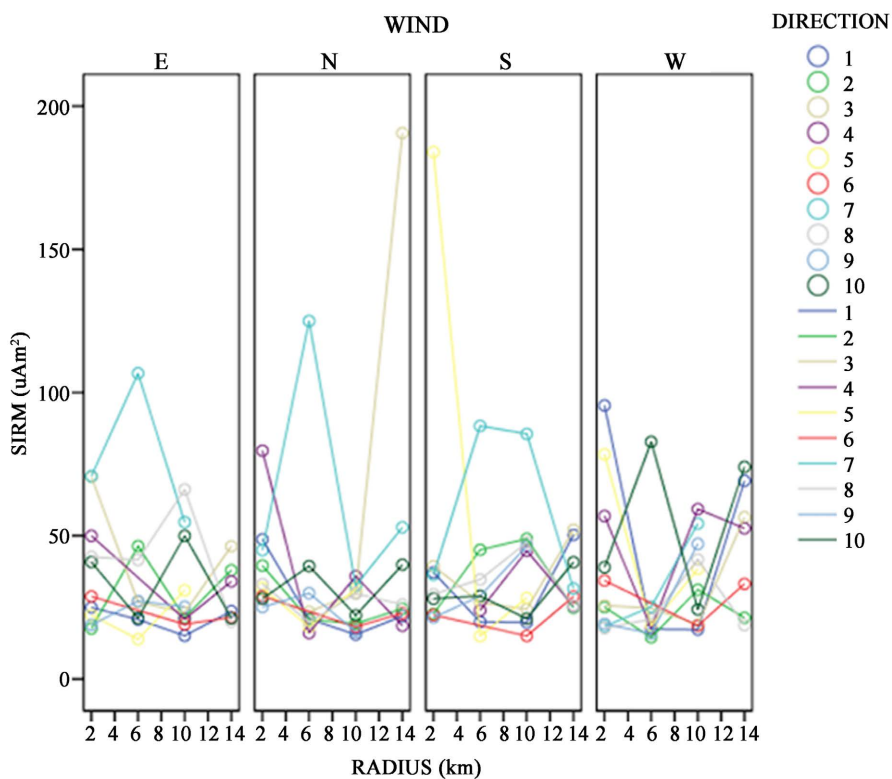
Figure 5. SIRM (unit: μA) of dust samplers over various directions, radial distances (unit: km) and azimuths (unit: E, N, S, W).

Figure 6. HIRM% of dust samplers at the four azimuthal positions (unit: E, N, S, W) and radial distances 2, 6, 10, 14 (unit: km).
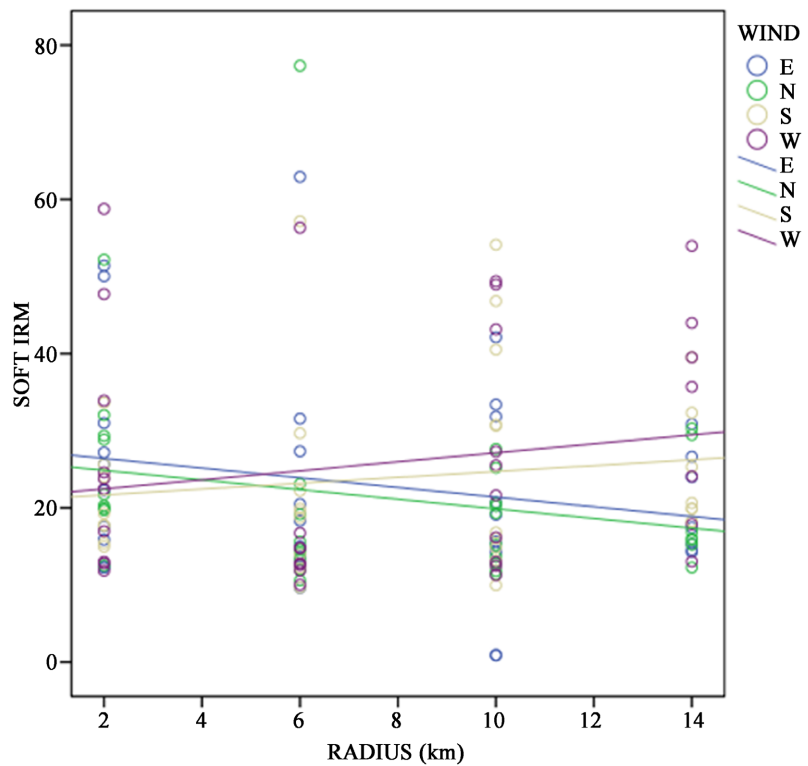
Figure 7. SOFT% of dust samplers at various radial distances (unit: 2, 6, 10, 14 km) and azimuths (unit: N, S, E, W).

Figure 8. Multiple linear regression graph indicating NRM (μA) of dust samplers over various radial distances (km).
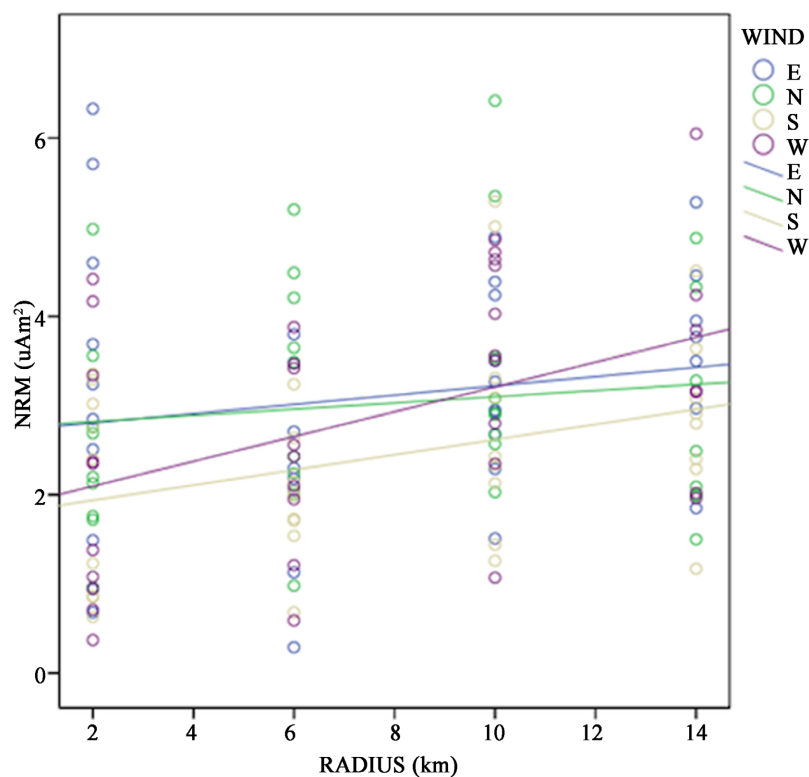
for all sampling directions ranged from 0.63 to 5.20 ± 1.47 μA. All directions exhibited similar NRM values with the exception of 236° indicating lower NRM values than 248° (ref) with a weak tendency, (p = 0.066). Dust sampler SIRM ranged from 34.43 to 190.57 μA. At 184° significantly higher SIRM values were determined than 248° (ref) (p < 0.001), as well as a significantly higher SOFT value (p < 0.01). A significant difference in Soft IRM% was displayed for 236° (p = 0.005) and 165° (p = 0.004) in comparison to 248° (ref). No sampling degree indicated a significant difference for s-ratio, although 165° displayed a suggestive trend (p = 0.060).

3.2. Azithumal Direction

NRM for dust samplers were; North ranged from 0.96 - 6.42 ± 1.27 μA, East from 0.29 - 6.33 ± 1.41 μA, South ranged from 0.63 - 11.01 ± 1.82 μA and West ranged from 0.37 - 6.05 ± 1.41 μA. Significant differences were determined between dust samplers depending on azimuthal direction, the south azimuths exhibited lower NRM values than the reference direction east (p = 0.022). For dust samplers SIRM values were highest from the North (190.57 μA) > E (106.71) > S (183.95) > W (95.46). Dust samplers west azithumal direction showed higher s-ratio than the east (p = 0.013). There was a strong tendency regarding the west azithumal direction as it exhibited higher Hard IRM% than east (ref) (p = 0.080) (Figure 3). North wind direction showed lower soft IRM% than East (ref) (p =

0.066) (Figure 4).

3.3. Correlation between Magnetic Parameters and Substrates

For dust sampler radial distance, sampling degree and azithumal direction accounted a significant amount of variation of NRM (p = 0.011; R^2 = 0.184), SIRM (p = 0.001; R^2 = 0.223) and s-ratio (p = 0.044; R^2 = 0.166), Soft IRM (p = 0.006; R^2 = 0.197) and Soft IRM% (p = 0.001; R^2 = 0.226). The percentage of total variation by factors is 78.7%, there are five factors that justify the 78.7% of common variance between the 14 magnetic parameters, and this demonstrates a moderately high strength of correlation between parameters (Table 1). The first factor accounted for 22.6% of the variance relative to the total variance in all the variables. The second factor 17.6%, the third factor 15.6%, the fourth factor 14.9% and the fifth factor 7.9% (Table 1).

Finally, the rotated factor matrix provided partial correlations between magnetic parameters and sampling material that are necessary to interpret the factors (Table 2). The 1st dimension positively correlates hard IRM and hard IRM (%) and both negatively with s-ratio, all these parameters are measured for *P. dactylifera*. The 2nd dimension positively correlates levels of SIRM, hard and soft IRM for dust samplers. The 3rd dimension negatively correlates levels of s-ratio and hard IRM (%), both for dust samplers. The 4th dimension positively correlates levels of SIRM and SOFT, both for *P. dactylifera*. The 5th dimension corresponds

Table 1. Variance and cumulative variance of azithumal direction of dust sampler and *P. dacterfylia* using unweighted least squares (ULS) and Varimax rotation.

| Factor	Initial Eigen values			Extraction sums of squared loadings			Rotation sums of squared Loadings		
	Total	% of variance	Cumulative %	Total	% of variance	Cumulative %	Total	% of variance	Cumulative %
1	3.843	27.450	27.450	3.745	26.750	26.750	3.168	22.631	22.631
2	2.519	17.996	45.446	2.440	17.428	44.178	2.471	17.650	40.281
3	2.347	16.761	62.207	2.284	16.314	60.492	2.178	15.559	55.840
4	1.884	13.454	75.662	1.713	12.233	72.724	2.081	14.863	70.703
5	1.061	7.580	83.241	0.833	5.923	78.676	1.116	7.973	78.676
6	0.858	6.129	89.370						
7	0.757	5.405	94.776						
8	0.454	3.243	98.019						
9	0.181	1.291	99.311						
10	0.088	0.629	99.940						
11	0.004	0.031	99.971						
12	0.003	0.019	99.990						
13	0.001	0.010	100.000						
14	−4.08E−07	−2.92E−016	100.00						

solely to the SOFT% for *P. dactylifera*. It should be noted that each different dimension only included parameters of the same sampling material: 1st *P. dactylifera*, 2nd dust sampler, 3rd dust samplers, 4th *P. dactylifera* and 5th *P. dactylifera*.

3.4. Distribution Pattern and Source Identification through Mapping

The predicted surfaces spatial distribution of magnetic parameters and inter-parametric ratios indicating the concentration, mineralogy, and grain size of magnetic minerals present in Kuwait for the duration of the study is illustrated in Figures 9-15. There were some similarities in the spatial distribution patterns

**Table 2.** Factorial analysis rotated factor matrix indicating partial correlations between magnetic parameters and sampling material.

	Factor				
	1	2	3	4	5
NRM dust sampler	0.495	−0.104	0.161	0.90	−0.088
SIRM dust sampler	−0.66	0.972	−0.122	−0.186	0.123
s-ratio dust sampler	0.140	−0.090	−0.902	0.124	−0.016
Hard IRM dust sampler	−0.044	0.741	0.398	0.140	0.017
Soft IRM dust sampler	−0.056	0.896	−0.178	−0.232	0.158
Hard IRM% dust sampler	−0.063	−0.022	0.960	−0.093	0.041
Soft IRM% dust sampler	0.143	−0332	−0.107	−0.130	0.067
NRM *P. dactylifera*	−0.40	0.013	0.278	−0.011	−0.206
SIRM *P. dactylifera*	0.036	−0.075	−0.111	0.984	−0.012
s-ratio *P. dactylifera*	−0.979	0.074	0.179	0.046	−0.039
Hard IRM *P. dactylifera*	0.975	−0.065	−0.180	0.034	0.051
Soft IRM *P. dactylifera*	0.020	−0.018	−0.115	0.952	0.281
Hard IRM% *P. dactylifera*	0.979	−0.074	−0.179	−0.046	0.039
Soft IRM% *P. dactylifera*	−0.026	0.153	−0.010	0.209	0.967

(a)   (b)

(c)

(d)

(e)

(f)
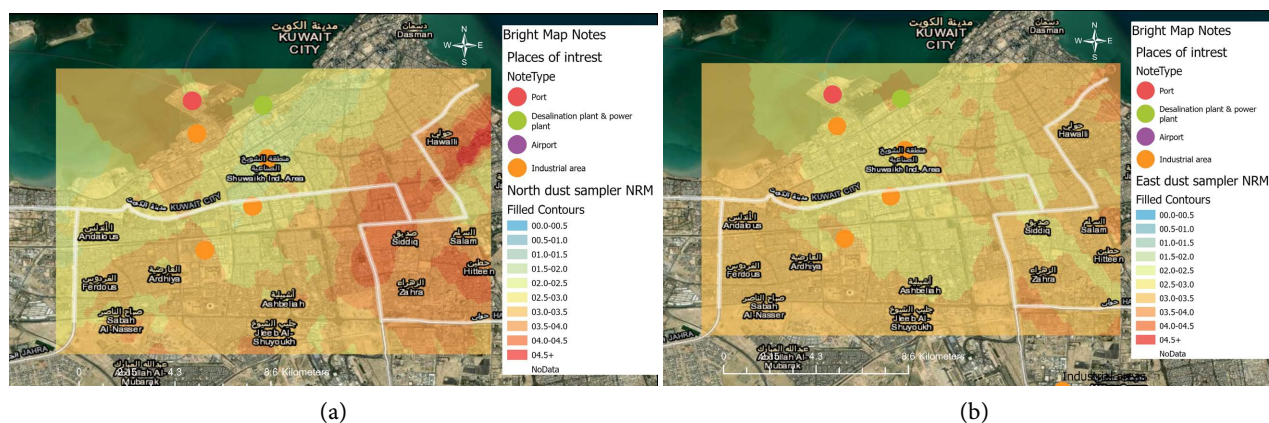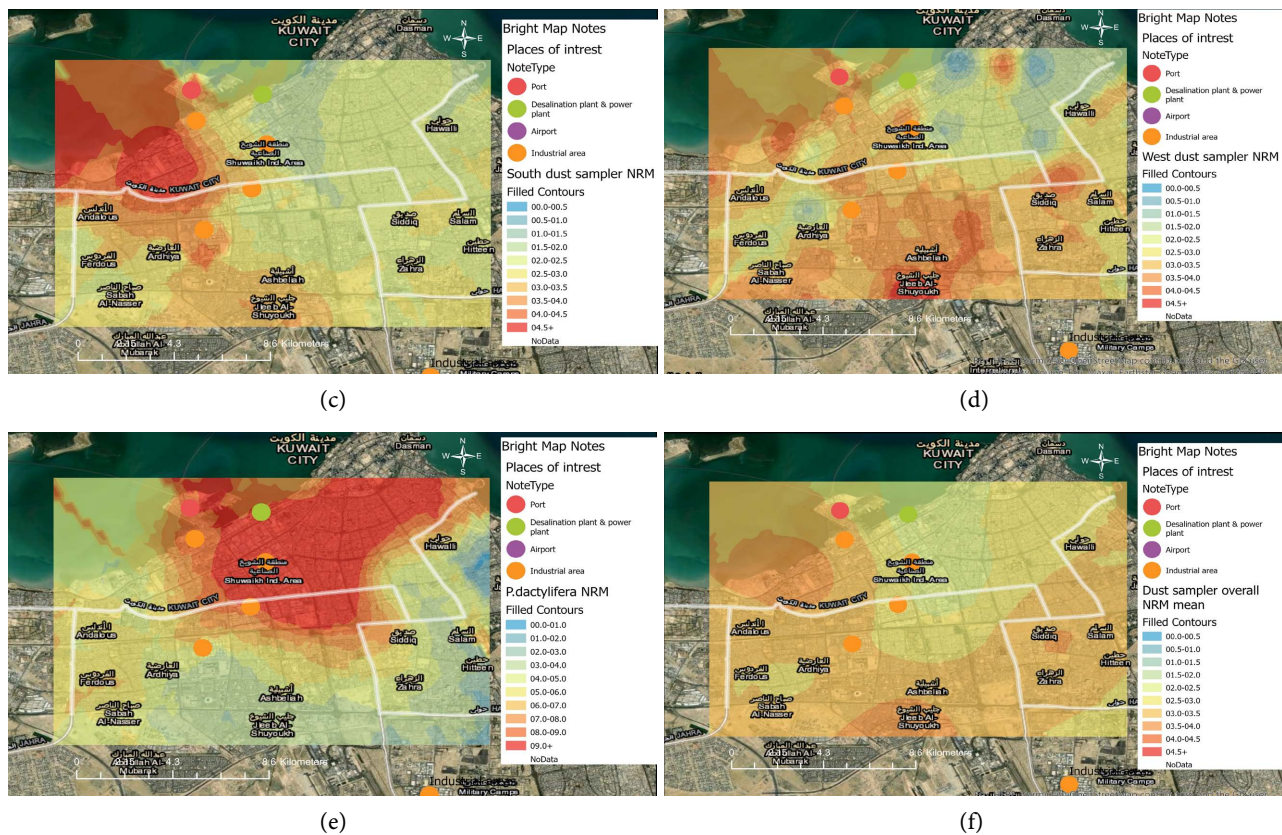
Figure 9. Spatial distribution mapping indicating NRM (unit: μA); (a) north, (b) east, (c) south, (d) west azithumal dust samplers and (e) *P. dactylifera*, (f) overall NRM mean for dust samplers.

(a)

(b)

(c)

(d)

(e)

(f)
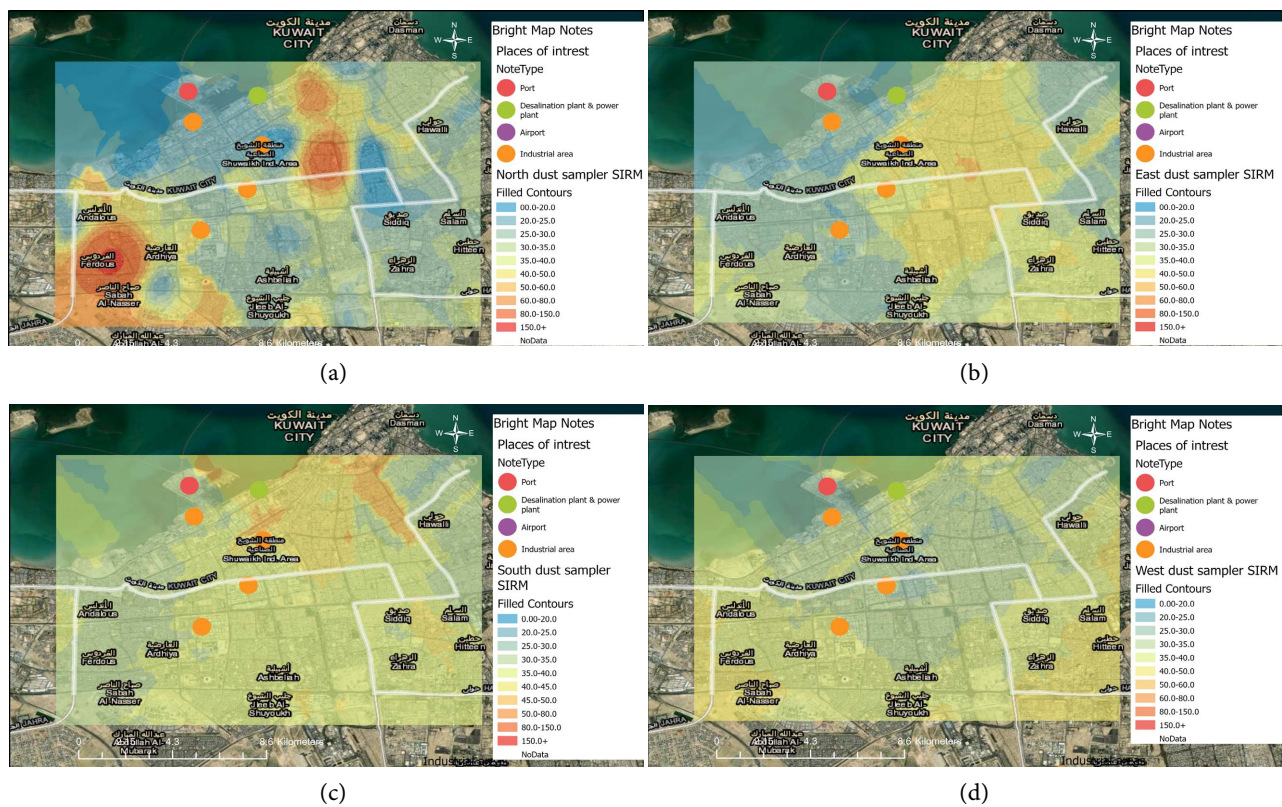
Figure 10. Spatial distribution mapping indicating SIRM (unit: μA); (a) north, (b) east, (c) south, (d) west azithumal dust samplers and (e) *P. dactylifera*, (f) overall SIRM mean for dust samplers.

(a)

(b)

(c)

(d)

(e)

(f)
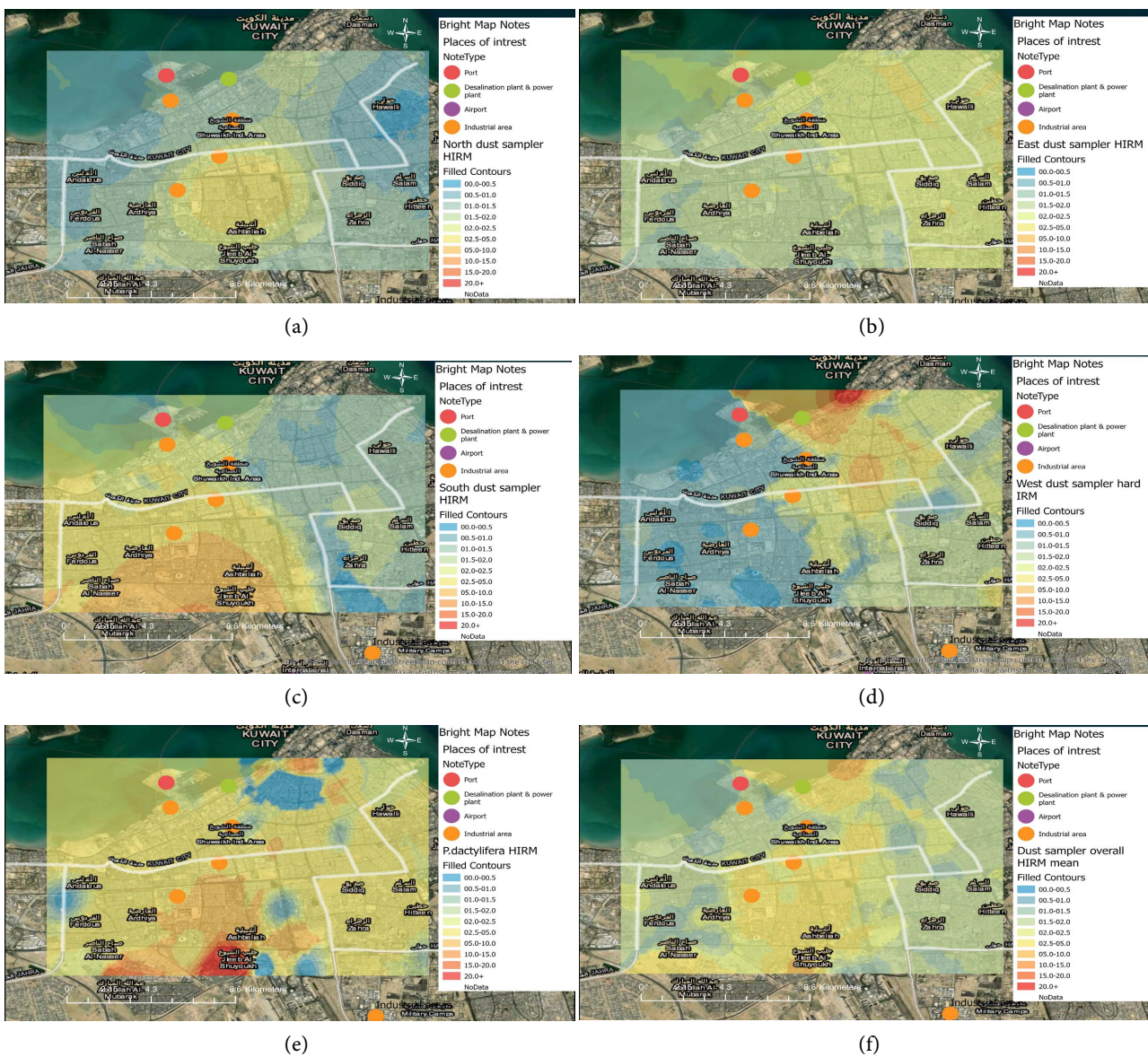
Figure 11. Spatial distribution mapping indicating HIRM (unit: μA); (a) north, (b) east, (c) south, (d) west azithumal dust samplers and (e) *P. dactylifera*, (f) overall HIRM mean for dust samplers.
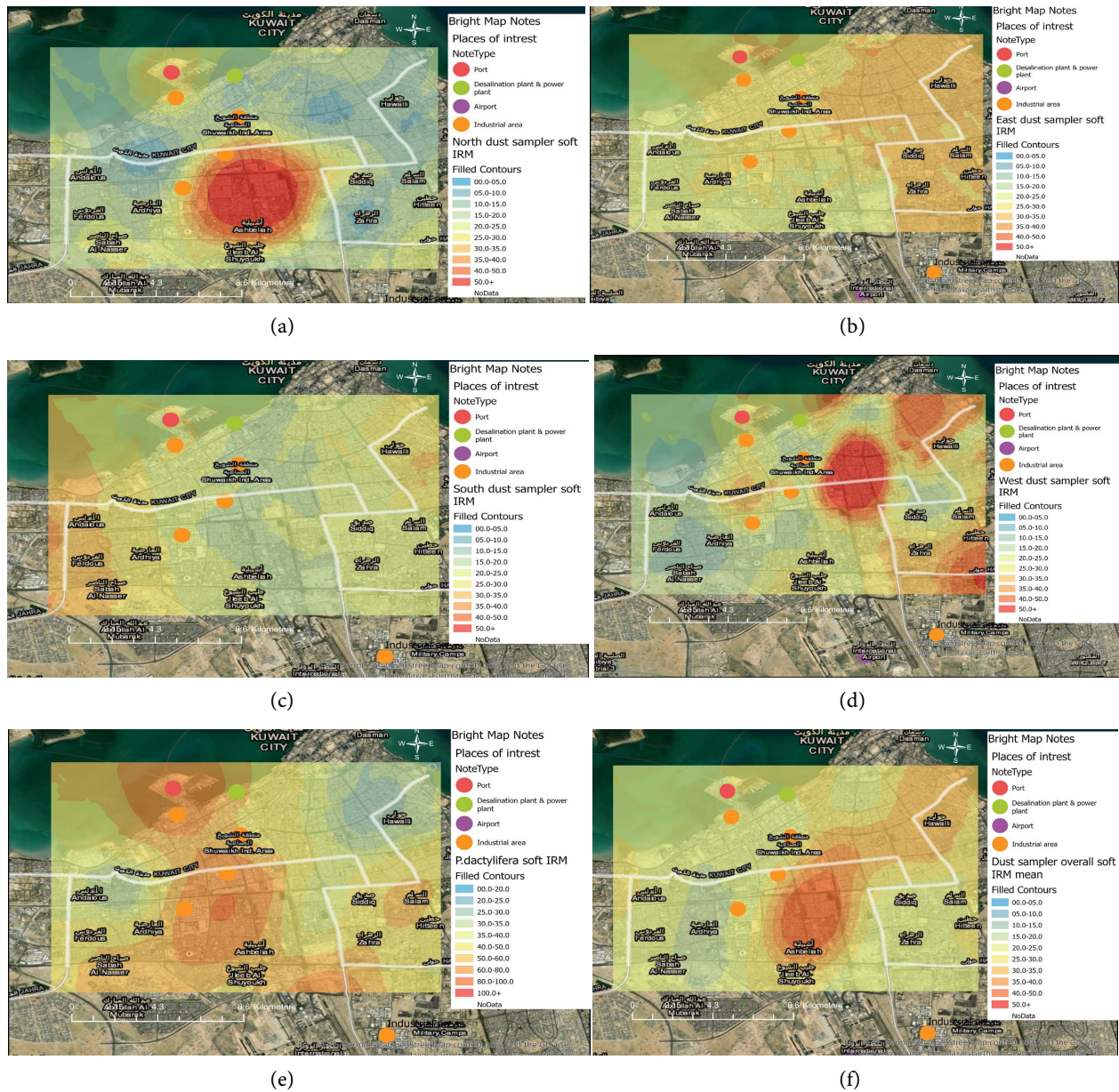
Figure 12. Spatial distribution mapping indicating soft IRM (unit: μA); (a) north, (b) east, (c) south, (d) west azithumal dust samplers and (e) *P. dactylifera*, (f) overall soft IRM mean for dust samplers.

(c)

(d)

(e)

(f)
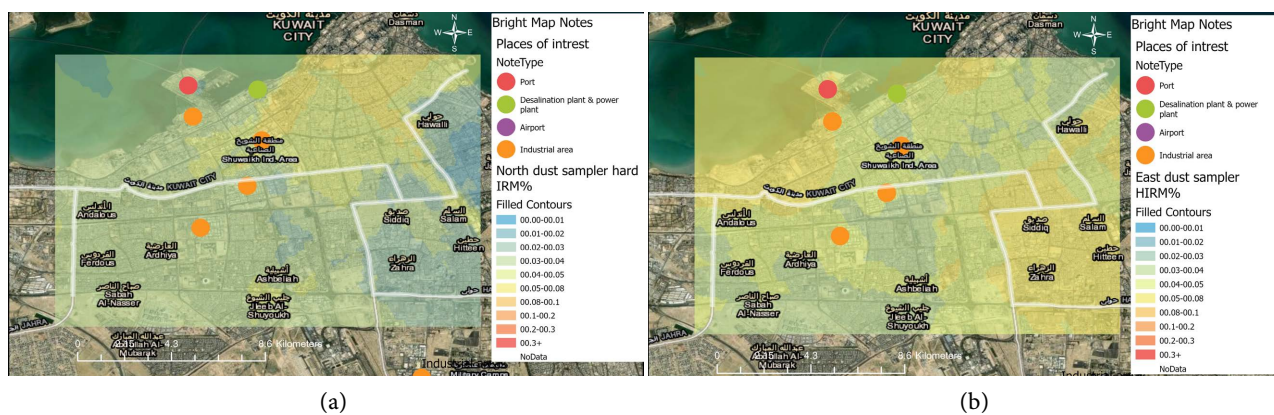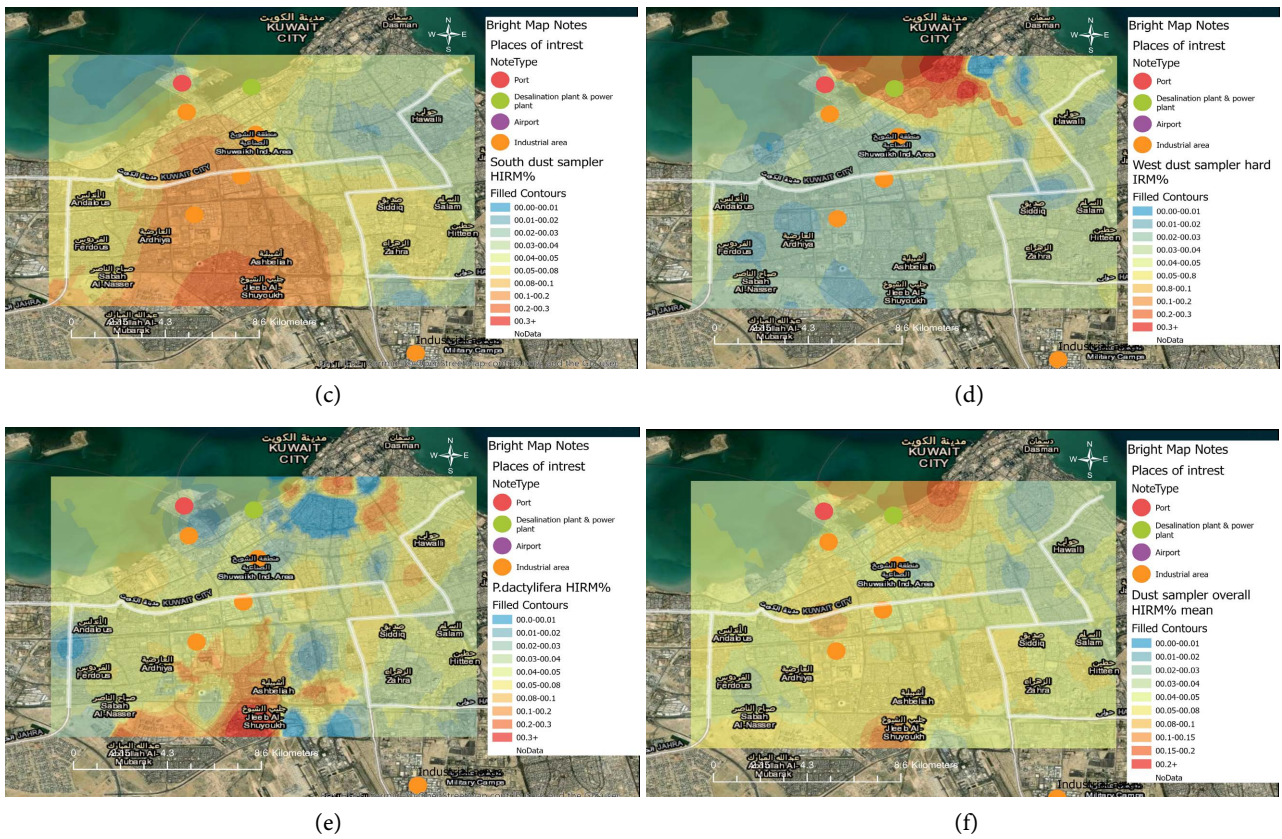
Figure 13. Spatial distribution mapping indicating HIRM%; (a) north, (b) east, (c) south, (d) west azithumal dust samplers and (e) *P. dactylifera*, (f) overall HIRM% mean for dust samplers.

(a)

(b)
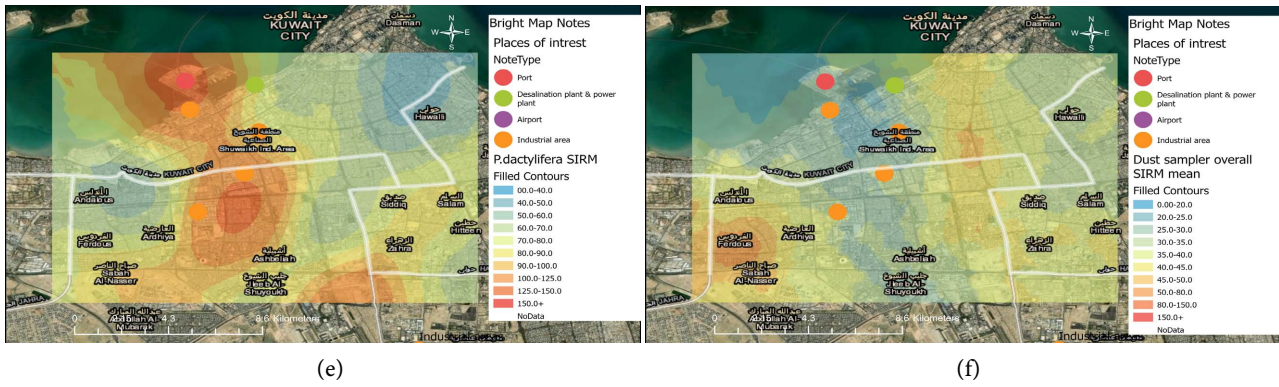

(c)

(d)

(e) (f)

Figure 14. Spatial distribution mapping indicating Soft IRM%; (a) north, (b) east, (c) south, (d) west azithumal dust samplers and (e) *P. dactylifera*, (f) overall Soft IRM% mean for dust samplers.

(a) (b)

(c) (d)

(e) (f)

Figure 15. Spatial distribution mapping indicating *s*-ratio; (a) north, (b) east, (c) south, (d) west azithumal dust samplers and (e) *P. dactylifera*, (f) overall *s*-ratio mean for dust samplers.
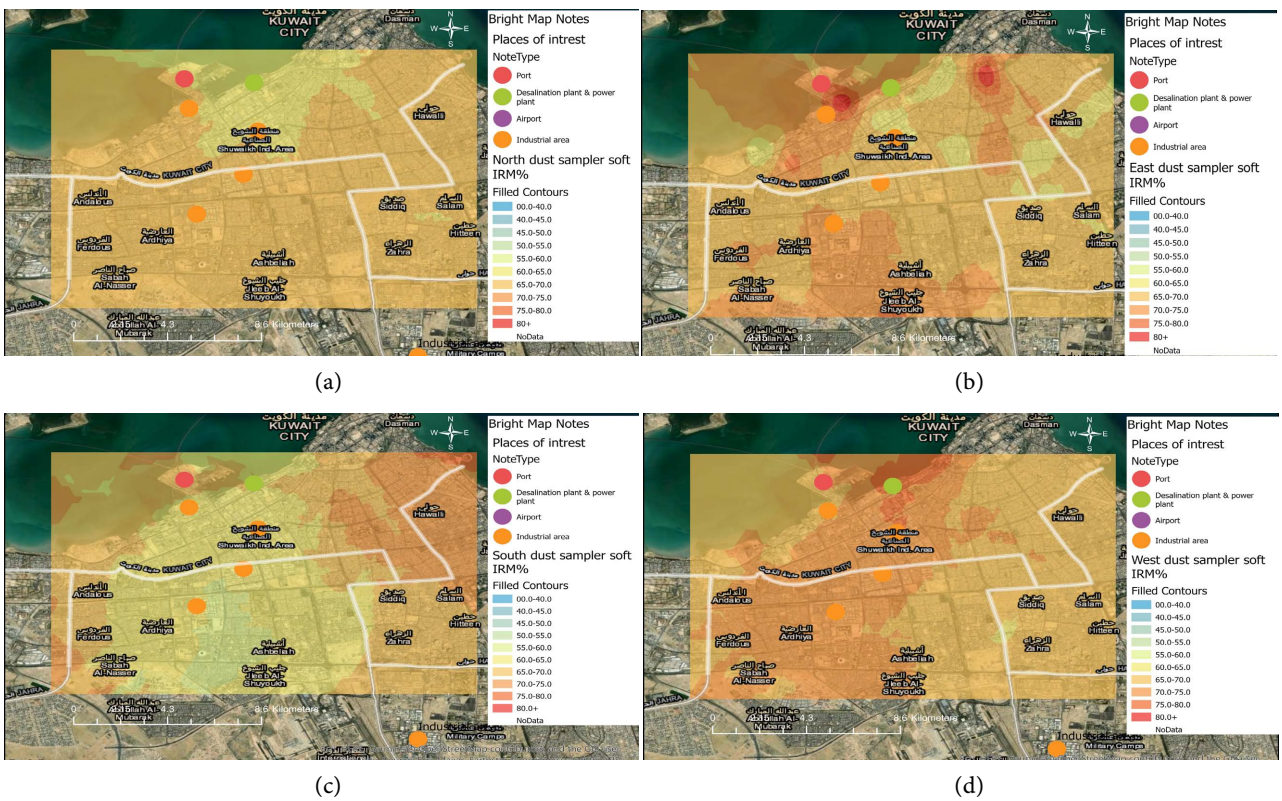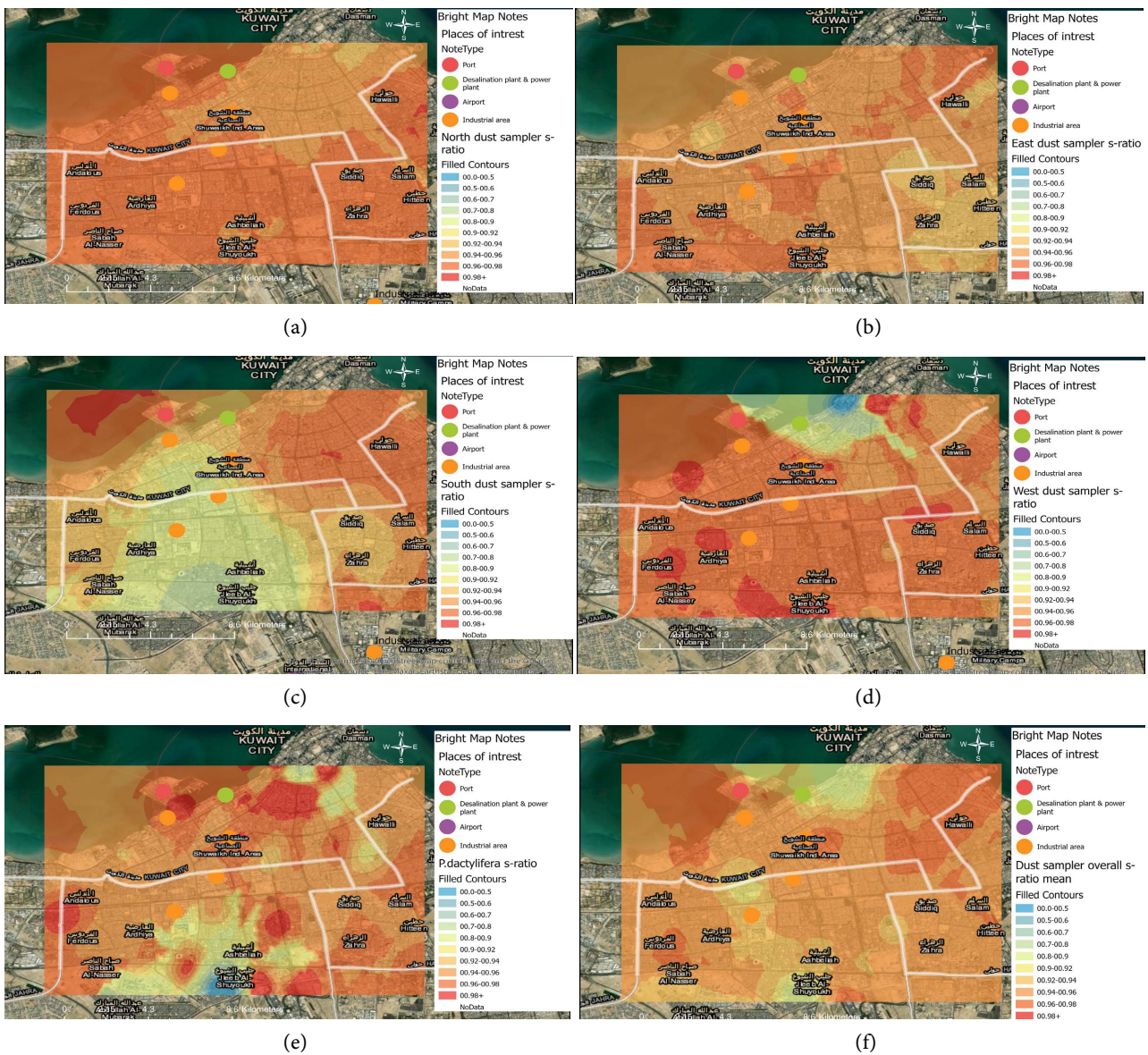
for soft IRM, HIRM, hard IRM% and *s*-ratio between active and passive biomonitoring methods and the overall mean of dust samplers.

4. Discussion

4.1. Pre-Treatment

Mean (NW) *P. dactylifera* values at the 2 km were higher than (NW) values for NRM, SIRM, soft IRM and *s*-ratio by 56%, 16.5%, 15.11% and 3% respectively. While, HIRM, soft IRM%, and HIRM% of (NW) *P. dactylifera* were lower by −35.6%, −1.3% and −68.8%, respectively. SIRM at the 2 km radial distance at every sampling point, was determined to be close to statistical significance for *P. dactylifera* (W) and (NW) (p = 0.064). The efficiency of washing or cleaning leaf surfaces in the removal of particulate matter fractures is dependent on the cleaning or washing procedure, some studies rinse samples for 30 minutes using deionized water [41] [42] [43]. Regardless, the standardization of (W) *P. dactylifera* in comparison to dust sampler will vary as some concentrations of elements in plant tissues can be technically affected by; the soil or substrate they are growing on, interspecies differences, vegetation effects, altitude and proximity to the source [41]. The washing procedure offers one great advantage which is the elimination of soil-relation effect [42]. Aboal *et al.* (2011) found evidence that by washing moss, *Pseudoscleropodium purum* (Hedw.) M for 30 seconds does not completely remove all of the particles deposited on the moss surface [44]. This is further supported by Bustamante *et al.* (2015) results that suggest that there is a potential link between the sources of the PAHs found in particles attached to mosses and of those bioconcentrated in their tissues as concentration of PAHs in both washed and non-washed were affected in relation to the emission source [43]. However, a study on the use of washed and unwashed *P. dactylifera* leaves as a biomonitor for Fe, Pb, Zn, Cu, Ni, and Cr concentrations in Ma'an city, Jordan determined that the amount of metals in the investigated area removed from the leaves by washing differed greatly depending on the contaminant level at each studied area, ex. 24% - 60% of the lead was removed by the washing process [44].

4.2. Comparison of Passive and Active Biomonitoring

Magnetic susceptibility was negligible in both biomonitoring techniques, this can be contributed to magnetic susceptibility being more suited to higher magnetic materials (e.g. soil and rock) and that diamagnetic minerals quartz, calcium carbonate, feldspar and calcite enrich in Kuwait's dust [45] [46] [47] [48]. Kuwait's soils are classed "silt loam" and "silt" with a size fraction of (2 - 62.5 μm), containing less than 10% clay [49]. According to Al-Awadhi & AlShuaibi (2013), grain size percentages vary between the city and the open desert, open desert dust consists of 63% fine particles and 37% coarser particles of the total dust samples, while Kuwait city's dust consist 39% fine and 56% coarse particles [37]. Similar mineralogy's are displayed across soils across various sites in Ku-

wait they are made-up of (27% and 54%) quartz, (~21%) plagioclase feldspar, (~10% - 20%) calcite, smaller amounts of clay minerals (palygorskite, illite-montmorillonite, and smaller amounts of kaolinite and little, if any, dolomite [46] [48]. Montmorillonite and palygorskite have elements Al, Fe, Ti and Mn that occur together or attached to them [49]. Small induced magnetizations are acquired by diamagnetic materials, which align opposite to the applied field direction, diamagnetic substances include; water ($X \sim -0.9 \times 10^{-8}$ m^3·kg^{-1}), quartz ($X \sim -0.6 \times 10^{-8}$ m^3·kg^{-1}), and calcium carbonate ($X \sim -0.5 \times 10^{-8}$ m^3·kg^{-1}) [46]. These low susceptibility values of <2.0 are an indication of virtually no or <10% SP grain in samples as a result of dust probably having substantial paramagnetic and diamagnetic contributions. Whereas, ferrimagnetic fractions with higher paramagnetic/diamagnetic contributions are considered as lithogenic if anthropogenically produced magnetic fractions do not significantly dominate those contributions [47]. Re-suspended dust samples from the Middle East have a Fe/Al ratio range of (Fe/Al = 0.87 - 1.38) PM$_{10}$ and (Fe/Al = 0.74 - 1.10) for PM 2.5 [49]. Fe and Al are predominantly in chemical forms of oxide in species and residual forms probably from the oxides and silica of the land, therefore a lithogenic contribution can be assumed [49] [50]. However, because of the low contribution of iron oxide from the parent rock, the χ lf value of all studied sample were considerably low leading to the conclusion that magnetic minerals all studied samples are predominantly contributed by different anthropogenic sources and not lithogenic or pedogenic ones [51] [52].

For passive biomonitoring *P. dactylifera* had an overall maximum SIRM average of 155.08 ± 35.74 μA. Similar findings were observed by Van Wittenberghe *et al.* (2013) for *Phoenix canariensis*, which was determined to have a maximum SIRM average of (189 ± 49) × 10^{-6} A [53]. While active biomonitoring, dust samplers values were lower accounting for a 36% difference in mean SIRM values between (W) *P. dactylifera* and dust samplers and a 54% difference for (NW) *P. dactylifera*, suggesting passive biomonitoring through the use of *P. dactylifera* accumulates a higher number of ferrimagnetic material than active biomonitoring using dust samplers. The difference in SIRM values is due to *P. dactylifera* leaves undergoing longer exposure duration time, in comparison to dust samplers period of 2 weeks as well as wax encapsulation. These observations coincide by Declercq *et al.* (2020) that interpolated active (strawberry) and passive (grass) biomagnetic monitoring methods revealed enhanced SIRM values distinctive for industrial areas in comparison to (passive) plastic coated cardboards (PCCs) biomagnetic monitoring that did not allow to accurately delineate a clear spatial pollution trend because of the smooth sampling surface resulting in the majority of SIRM values not to exceeded 50 μA [54]. These observations are further supported by Barima *et al.* (2016), three ornamental species (*Jatropha interrigima*, *Ficus benjamina* and *Barleria prionitis*) in Abidjan (Ivory Coast) were evaluated for PM retention and it had been determined that leaf SIRM values were higher on mature leaves suggesting the accumulation of particles in

leaves over time especially in waxy species (*Ficus benjamina*) as PM is encapsulated in the wax structure over the growing season [30].

Both (NW) *P. dactylifera* and dust sampler have considerably higher SOFT values than HIRM values, with mean HIRM at 2.81 μA, and 3.01 μA, where as SOFT values were 176% and 163% higher, respectively. Both (NW) *P. dactylifera* and dust samplers have considerably higher values of Soft% than hard IRM%, with soft% making up 58.7% of SIRM for (NW) *P. dactylifera* and 67.8% for dust samplers. Xia *et al.* (2012) determined that there is a linear correlation between SIRM and SOFT for surface soil samples which suggests that they are dominated by ferrimagnetic minerals, as IRM of surface samples were around 98% of the SIRM at magnetic field of 300 mT, implying that low coercivity magnetite and maghemite dominant the remanent magnetization of the samples [55]. This signifies that magnetic minerals in Kuwait are dominated by ferrimagnetic mineral of anthropogenic origin that exhibit soft magnetic behavior, with low coercivity, that are in the multidomain (MD) range, with a grain size of (>10 - 15 μm) and at the superparamagnetic/stable single domain (SP/SD) border (80 nm - ~10 - 15 μm) [56] [57]. As magnetic iron oxide is associated to large number of magnetic particles that are released from traffic emission, industrial activities and fuel combustions they act by a preferential adsorption with heavy metals Pb, Zn, Cu, Cr, Cd on the surface of iron (III) oxyhydroxides or present in the form of substituted spinels of $Fe_{3-x}M_xO_4$, this enables magnetic measurements to order to monitor environmental pollution [58]. Magnetic iron oxides are associated to a large number of magnetic particles that are released from traffic emission, industrial activities and fuel combustions they act by a preferential adsorption with heavy metals Pb, Zn, Cu, Cr, Cd on the surface of iron (III) oxyhydroxides or present in the form of substituted spinels of $Fe_{3-x}M_xO_4$.

Low HIRM% values for (NW) *P. dactylifera* and dust samplers average at 3.77% and 6.57%, an indication of fairly low concentration of hematite/goethite. This data is comparable to modern African soil samples from Niger, Morocco and Tunisia sampled as potential dust sources that displayed a $HIRM_{100\%}$ between 8% and 32% [46] [59] [60]. This implies that low coercivity multidomain (MD) ferromagnetic minerals (magnetite) dominate the magnetic properties of PM, while incomplete anti-ferromagnetic minerals make up a low proportion [61]. Natural sources are reflected through hard IRM%, this is possibly due to the formation of hematite favoring drier climates with low water content and high temperatures owing to the dehydration ferrihydrates [62] [63] [64]. The presence of ferrimagnetic mineral components dominating the samples is further confirmed as *s*-ratios were close to 1 reaching almost to unity over all samples, as low *s*-ratio is identified as haematite, high *s*-ratio is greigite [65].

A relationship between radial distance and NRM for *P. dactylifera* was observed, with NRM values dropping as radial distance increased, moving away from the highly urbanized city center and the coast towards more suburban, industrial areas. The relationship between magnetic intensity and land use corres-

ponds with Kardel *et al*. (2012) and Mitchell and Maher (2009) findings that noted that SIRM is lower in less urbanized land classes in comparison to central city areas that experience a higher intensity of traffic [22] [45]. The opposite was found for HIRM% as values declined with radial distance this may signify that there are different sources away from the city center and/or mixing with other sediment magnetic components [46]. Radial distance significantly correlated with *s*-ratio, Hard IRM% and soft IRM% and xFD(%) for dust samplers. All these parameters increased as distance increased in a linear pattern. Only for dust samplers were there some specific correlations in regards to sampling degrees. For example, with direction 9 suggesting higher values of NRM, HF and LF in comparison to reference (direction 1) over radial distances of 2, 10, 14 km. Indicating a longitudinal pattern from the city center outwards that may be affected by the airport that within the vicinity.

Correlations between SIRM, HIRM and SOFT magnetic concentration for dust sampler in this study were R^2 values are above 0.7. It is clear that high values of χ_{lf}, SIRM, SOFT are identified as magnetite concentration-related parameters and are linked to high element concentrations that arise from high temperature fossil-fuel combustion processes, vehicles, power plant and cement plant operations, building and road surface materials (e.g., metallic fragments, slag and building materials) [57] [59] [63]. These results coincide with findings on the correlation of magnetic properties and heavy metals content in urban soils of Hangzhou City, China (Lu & Bai, 2006), that identified that there is a significant correlation that exists between Cu, Zn, Cd and Pb and χ, ARM, SOFT and SIRM, demonstrating the presence of heavy metals and magnetic particles MD grains that are of anthropogenic origin [57]. These results are also consistent with findings from Wang *et al*. (2012) that χ_{lf}, SIRM, SOFT, and HIRM, as well as S-300 are linked to relatively greater hematite contributions along with As, Ba, Mn, Cu, Pb, Fe and Ti [59]. However it must be noted, that the factorial analysis showed that there was no relationship between magnetic parameters obtained from dust samplers and those from *P. dactylifera.* It may be assumed that the difference in values may be a result of exposure time, surface morphology, as well as the fact that leaf contents sum up from depositions, root uptake and also by seasonal differences in emissions influencing PM accumulation rate [25] [66].

4.3. Azithumal Direction

The effect of azithumal direction was tested using the dust samplers to test the effect of azithumal sampling degree at each sampling location impacted magnetic parametric readings. It was observed that the prevailing wind direction (NW) at 8 - 10 m/s coincide with the direction in which exhibited the highest SIRM values for dust samplers, SIRM were highest from the North (190.57) > E (106.71) > S (183.95) > W (95.46). *s*-ratio and HIRM% were also highest in the west azithumal direction indicating that the azimuthal position of where a sam-

ple collected causes a NRM, SIRM, *s*-ratio soft IRM% variations. Mass concentration of total suspended particles (TSP), PM10, PM 10 - 2.5 fractions are affected by meteorological parameters; wind speed, wind direction, rainfall and temperature [67]. Dust events in the Middle East are determined to have relatively weak wind speeds that can reach 10 ms causing dust-in-suspension to predominantly to occur [68]. These findings concede with Hofman *et al.* (2013) results in the assessment of the spatial distribution of particulate matter of deposited particles on tree crowns in an urban street canyon that determined that air circulation caused azimuthal effects and that it is directly influenced by street architecture, as individual tree crowns indicated an azimuthal leaf SIRM variation (p = 0.0446) depending on their position in a street canyon [69]. Hofman *et al.* (2013) found that all edge trees that were exposed to intense air circulation were determined to have the lowest SIRM values at the windward side of the tree crown (NW-SW), whilst the highest leaf SIRM values were at the leeward sides of the tree crown (NE, SE) as changing airflows increase of impaction and interception of particles causing azimuthal SIRM variations [69]. This is further confirmed by a study conducted by Zhang *et al.* (2008) on Chinese willow (*Salix matsudana*) tree ring cores, that suggests that magnetic particles enter into the xylem during the growing season as tree ring cores facing the pollution source displayed higher SIRM than other sides of the tree [70]. It must be noted further research needs to conduct on the comparison of azithumal effects between *P. dactylifera* (active) and dust sampler (passive) biomonitoring effects over a long duration of time to see if the amount of deposited magnetic particles differed at similar azithumal degrees or whether they reach equilibrium.

4.4. Distribution Pattern and Source Identification through Mapping

Interpolation of data has enabled more insight into the spatial distribution and behaviors of pollutants in the area as it included all input points including the outliers. However the magnetic maps may not be true spatial representatives of the local concentrations as previous studies that have used kriging to map PM have observed that by mapping large geographical areas with large distances between monitoring sites to have reduced reliability in the predicted values [71]. As seen on the maps there were some similarities in the spatial distribution's trends of soft IRM, HIRM, hard IRM% and *s*-ratio between active and passive biomonitoring methods and the overall mean of dust samplers. Passive biomonitoring offers more information on long term deposition rates and pinpoints hot spots and PM sources in comparison to active biomonitoring that offers more short-term PM deposition accumulation rate and behaviors in relation to meteorological conditions during the sampling time [54].

The azithumal direction in which the dust samplers were placed gave distinct results this may be a result of varying infrastructure across the area as well as building height and wind direction (**Figures 11-13**). The magnetic outcomes for

dust samplers follow a similar pattern to the wind trajectories. The highest concentration appeared in Kuwait City as well near the vicinity of industrial areas, ports and power plants and desalination plants and their surrounding area. As industrial hotspots and dense residential areas with high vehicular traffic tend to be exposed to higher PM 2.5 concentrations [72]. The prevailing wind direction during the sampling was northwest, the decrease in SIRM and NRM values and spread in maps can be attributed to the prevailing wind direction especially when comparing dust samplers to *P. dactylifera* (Figure 9 & Figure 10). The transportation, dispersal and dilution of air pollution are actively impacted by local winds, high amounts of air pollutants particularly from pointary or linear sources that produce high proportions emissions, to receptors or samplers at distinct wind directions [67]. Al-Nassar *et al.* (2005) determined that wind power density (WPD), that is defined as the frequency distribution of wind speed and the dependence of wind power on air density and the cube of the wind speed, expressed in Watt per square meter (W/m^2), in Kuwait is lower at the bay and increases outwards into open flat desert areas in the northern, northwestern and southern parts of the country, such as Al-Wafra, Al-Taweel and Umm Omara, indicating that wind direction has a significant effect on daily magnetic mineralogizes and grain size [73]. Prevailing wind direction is seen to impact, magnetite concentration to a range of 0.24% - 0.89% at distance of 500 m away from cement plants, while decreasing to a concentration of 0.02% to 0.16% at a distance of 3 km or more [74]. As well as parallel MS profiles measured perpendicular to road surfaces at a distance of 20 m on either side of a road have been determined to be a reflection of clear symmetry to prevailing winds [75]. A study on pollution utilizing roadside plant leaves in an Indo-Burma hot spot region found that plants showed higher magnetic concentrations in sites with poor roads that experience heavy traffic, street dust load and tall buildings that tend to concentrate pollutants as there is lower rate of PM dispersal [76]. As wind flow patterns can be skewed in cities with individual or groups of buildings, governing the interaction between the flow and buildings in the vicinity and local air pollutant dispersion [77]. Further research can address these limitations through the application of 3D spatial visualization that incorporates seasonal and meteorological analytics that can better help in the examination of local air circulation and its role in the dispersion and transport of PM throughout urban infrastructure.

The highest magnetic concentration values of NRM and SIRM for *P. dactylifera* occur near Kuwait bay, with the majority of urban infrastructure and PM sources located at the bay, the proximity of Kuwait Bay mandates the effects land and sea breeze impacting air flow and PM dispersion. In a previous study conducted by Engelbrecht *et al.* (2009) on magnetic measurements of dust samples collected on Nuclepore filters it was determined that coastal Kuwait samples are 3 to 5 times more magnetic, in comparison to other locations [78]. Higher SIRM values are distinct for dust sampler although its more distinct in Kuwait City in comparison to *P. dactylifera* which has high SIRM values generating from the Kuwait bay area inwards (Figure 10). The soft diamagnetic behavior was found

to be similar to North of Kuwait, while the central and southern dust samples were distinctive by their 'hard', haematite-like behavior [78]. This could be as a result of an association between lithogenic origins of soil, organic matter content and certain magnetic properties of urban street dust that may vary due to lithogenic origins depending on varying locations within an area and roads [79] [80].

The maps clearly demonstrate that dust samplers although time consuming are suitable method in the determination of short-term PM pollution distribution patterns that are heavily influenced by prevailing wind directions, while *P. dactylifera* offers corresponding information towards determining long term PM pollution patterns, hot spots and sources. The reliability of these predictions would thoroughly be improved in further research through the addition of meteorological influences to the predicted values to better discriminate magnetic particles dispersal patterns [72].

5. Conclusion

The outcome of this study validates the utilization of both *P. dactylifera* and dust samplers as proxies for PM pollution. The outcome of magnetic parameter data of both the passive and active biomonitoring techniques was similar in certain aspects in that the magnetic properties of Kuwait's PM *P. dactylifera* and dust samplers were both dominated by ferrimagnetic minerals (magnetite) from anthropogenic sources with low coercivity in the multidomain (MD) range and at the superparamagnetic/stable single domain (SP/SD) border with a grain size of (>10 - 15 μm) and (80 nm - ~10 - 15 μm) that may be influenced by the prominence of quartz, calcite in resuspended soil. Quartz, calcium carbonate, feldspar and calcite in Kuwaits dust and *P. dactylifera* leaf material have a diamagnetic behavior that may have resulted in very low magnetic susceptibility values. Similar results between both techniques were found for radial distance moving away from the city center and sampling degree. Radial distance affected NRM and HIRM for *P. dactylifera* and NRM for dust samplers. The analyses on the effects of azithumal direction of dust samplers indicated that wind direction influenced greatly, specifically in the northwest direction for the study period. The influence of wind direction, the position of Kuwait's bay and urban infrastructure was greatly highlighted through the application of simple kriging enabling interpolation to predict the spatial distribution of magnetic mineral concentrations and grain sizes in other sites of interest that were clearly better observed when mapped yet were not apparent in the statistical analysis. Geomagnetic spatial maps are proven to be a less tumultuous task and more economically efficient in comparison to geochemical analysis, particularly on a grand scale.

Acknowledgements

sisting in sample collections and lab preparations.

Conflicts of Interest

The authors declare no conflicts of interest regarding the publication of this paper.

References

[1] Al-Hemoud, A., Al-Dousari, A., Al-Shatti, A., Al-Khayat, A., Behbehani, W. and Malak, M. (2018) Health Impact Assessment Associated with Exposure to PM_{10} and Dust Storms in Kuwait. *Atmosphere*, **9**, 6. https://doi.org/10.3390/atmos9010006

[2] Kampa, M. and Castanas, E. (2008) Human Health Effects of Air Pollution. *Environmental Pollution*, **151**, 362-367. https://doi.org/10.1016/j.envpol.2007.06.012

[3] Gao, Y., Nan, S., Zheng, G. and Gao, T. (2016) Experimental Study on the Effect of Humidification on the Pollution Characteristics of Particulate Matter in the Office. *Journal of Environmental Protection*, **7**, 1791-1801. https://doi.org/10.4236/jep.2016.712143

[4] Ettouney, H., Al-Haddad, A. and Saqer, S. (2012) Daily and Seasonal Changes of Air Pollution in Kuwait. *World Academy of Science, Engineering and Technology*, **6**, 32-36.

[5] Thorpe, A. and Harrison, R.M. (2008) Sources and Properties of Non-Exhaust Particulate Matter from Road Traffic: A Review. *Science of the Total Environment*, **400**, 270-282. https://doi.org/10.1016/j.scitotenv.2008.06.007

[6] Smith, J.P., Brabander, D.J., Panek, L.A. and Besancon, J.R. (2019) Enrichment of Potentially Toxic Elements in the Fine Fraction of Soils from Iraq and Kuwait. *Journal of Soils and Sediments*, **19**, 3545-3563. https://doi.org/10.1007/s11368-019-02286-7

[7] Abbasi, S., Keshavarzi, B., Moore, F., Hopke, P.K., Kelly, F.J. and Dominguez, A.O. (2020) Elemental and Magnetic Analyses, Source Identification, and Oxidative Potential of Airborne, Passive, and Street Dust Particles in Asaluyeh County, Iran. *Science of the Total Environment*, **707**, Article ID: 136132. https://doi.org/10.1016/j.scitotenv.2019.136132

[8] Tanaka, T.Y. and Chiba, M. (2006) A Numerical Study of the Contributions of Dust Source Regions to the Global Dust Budget. *Global and Planetary Change*, **52**, 88-104. https://doi.org/10.1016/j.gloplacha.2006.02.002

[9] Farahat, A. (2016) Air Pollution in the Arabian Peninsula (Saudi Arabia, the United Arab Emirates, Kuwait, Qatar, Bahrain, and Oman): Causes, Effects, and Aerosol Categorization. *Arabian Journal of Geosciences*, **9**, Article No. 196. https://doi.org/10.1007/s12517-015-2203-y

[10] Goudie, A.S. (2009) Dust Storms: Recent Developments. *Journal of Environmental Management*, **90**, 89-94. https://doi.org/10.1016/j.jenvman.2008.07.007

[11] El Raey, M. (2006) Air Quality and Atmospheric Pollution in the Arab Region. ESCWA/League of Arab States/UNEP, Regional Office for West Asia Report.

[12] Song, Z., Wang, J. and Wang, S. (2007) Quantitative Classification of Northeast Asian Dust Events. *Journal of Geophysical Research Atmospheres*, **112**, 1-8. https://doi.org/10.1029/2006JD007048

[13] Goudie, A.S. and Middleton, N.J. (2001) Saharan Dust Storms: Nature and Consequences. *Earth-Science Reviews*, **56**, 179-204. https://doi.org/10.1016/S0012-8252(01)00067-8

[14] Alolayan, M.A., Brown, K.W., Evans, J.S., Bouhamra, W.S. and Koutrakis, P. (2013) Source Apportionment of Fine Particles in Kuwait City. *Science of the Total Environment*, **448**, 14-25. https://doi.org/10.1016/j.scitotenv.2012.11.090

[15] Khalaf, F.I., Al-Kadi, A. and Al-Saleh, S. (1985) Mineralogical Composition and Potential Sources of Dust Fallout Deposits in Kuwait, Northern Arabian Gulf. *Sedimentary Geology*, **42**, 255-278. https://doi.org/10.1016/0037-0738(85)90047-8

[16] Al-harahsheh, S. (2020) Spatial and Seasonal Variations of the Particulate Matters (PM_{10}) at Selected Sites in the State of Kuwait. *Pollution Research*, **39**, 19-32.

[17] Abd El-Wahab, R.H. and Al-Rashed, A.R. (2010) Vegetation and Soil Conditions of Phytogenic Mounds in Subiya Area Northeast of Kuwait. *Catrina—The International Journal of Environmental Sciences*, **5**, 87-95.

[18] Al-awadhi, J.M., Al-dousari, A.M. and Khalaf, F.I. (2014) Influence of Land Degradation on the Local Rate of Dust Fallout in Kuwait. *Atmospheric and Climate Sciences*, **4**, 437-446. https://doi.org/10.4236/acs.2014.43042

[19] Al-Dousari, A.M. and Al-Awadhi, J. (2012) Dust Fallout in Northern Kuwait, Major Sources and Characteristics. *Kuwait Journal of Science and Engineering*, **39**, 171-187.

[20] Mitchell, R., Maher, B.A. and Kinnersley, R. (2010) Rates of Particulate Pollution Deposition onto Leaf Surfaces: Temporal and Inter-Species Magnetic Analyses. *Environmental Pollution*, **158**, 1472-1478. https://doi.org/10.1016/j.envpol.2009.12.029

[21] Wang, X., Lang, L., Hua, T., Zhang, C. and Xia, D. (2015) Geochemical and Magnetic Characteristics of Aeolian Transported Materials under Different Near-Surface Wind Fields: An Experimental Study. *Geomorphology*, **239**, 106-113. https://doi.org/10.1016/j.geomorph.2015.03.017

[22] Mitchell, R. and Maher, B.A. (2009) Evaluation and Application of Biomagnetic Monitoring of Traffic-Derived Particulate Pollution. *Atmospheric Environment*, **43**, 2095-2103. https://doi.org/10.1016/j.atmosenv.2009.01.042

[23] Hoffmann, V., Knab, M. and Appel, E. (1999) Magnetic Susceptibility Mapping of Roadside Pollution. *Journal of Geochemical Exploration*, **66**, 313-326. https://doi.org/10.1016/S0375-6742(99)00014-X

[24] Thompson, R. and Oldfield, F. (1986) Environmental Magnetism. Allen and Unwin, London. https://doi.org/10.1007/978-94-011-8036-8

[25] Ştefănuţ, S., Öllerer, K., Ion, M. C., Florescu, L.I., Constantin, M., Banciu, C., Manole, A., *et al.* (2021) Country-Scale Complementary Passive and Active Biomonitoring of Airborne Trace Elements for Environmental Risk Assessment. *Ecological Indicators*, **126**, Article ID: 107357. https://doi.org/10.1016/j.ecolind.2021.107357

[26] Wolterbeek, B., Sarmento, S. and Verburg, T. (2010) Is There a Future for Biomonitoring of Elemental Air Pollution? A Review Focused on a Larger-Scaled Health-Related (Epidemiological) Context. *Journal of Radioanalytical and Nuclear Chemistry*, **286**, 195-210. https://doi.org/10.1007/s10967-010-0637-y

[27] Mo, L., Ma, Z., Xu, Y., Sun, F., Lun, X., Liu, X., Yu, X., *et al.* (2015) Assessing the Capacity of Plant Species to Accumulate Particulate Matter in Beijing, China. *PLOS ONE*, **10**, e0140664. https://doi.org/10.1371/journal.pone.0140664

[28] Speak, A.F., Rothwell, J.J., Lindley, S.J. and Smith, C.L. (2012) Urban Particulate Pollution Reduction by Four Species of Green Roof Vegetation in a UK City. *Atmospheric Environment*, **61**, 283-293. https://doi.org/10.1016/j.atmosenv.2012.07.043

[29] Dzierżanowski, K., Popek, R., Gawrońska, H., Sæbø, A. and Gawroński, S.W. (2011)

Deposition of Particulate Matter of Different Size Fractions on Leaf Surfaces and in Waxes of Urban Forest Species. *International Journal of Phytoremediation*, **13**, 1037-1046. https://doi.org/10.1080/15226514.2011.552929

[30] Barima, Y.S.S., Angaman, D.M., N'gouran, K.P., Koffi, N.A., Tra Bi, F.Z. and Samson, R. (2016) Involvement of Leaf Characteristics and Wettability in Retaining Air Particulate Matter from Tropical Plant Species. *Environmental Engineering Research*, **21**, 121-131. https://doi.org/10.4491/eer.2015.120

[31] Urbat, M., Lehndorff, E. and Schwark, L. (2004) Biomonitoring of Air Quality in the Cologne Conurbation Using Pine Needles as a Passive Sampler—Part I: Magnetic Properties. *Atmospheric Environment*, **38**, 3781-3792.
https://doi.org/10.1016/j.atmosenv.2004.03.061

[32] Giordano, S., Adamo, P., Spagnuolo, V., Tretiach, M. and Bargagli, R. (2013) Accumulation of Airborne Trace Elements in Mosses, Lichens and Synthetic Materials Exposed at Urban Monitoring Stations: Towards a Harmonisation of the Moss-Bag Technique. *Chemosphere*, **90**, 292-299.
https://doi.org/10.1016/j.chemosphere.2012.07.006

[33] Aboal, J.R., Pérez-Llamazares, A., Carballeira, A., Giordano, S. and Fernández, J.A. (2011) Should Moss Samples Used as Biomonitors of Atmospheric Contamination Be Washed? *Atmospheric Environment*, **45**, 6837-6840.
https://doi.org/10.1016/j.atmosenv.2011.09.004

[34] da Costa, G.M., Petry, C.T. and Droste, A. (2016) Active versus Passive Biomonitoring of Air Quality: Genetic Damage and Bioaccumulation of Trace Elements in Flower Buds of *Tradescantia pallida var. purpurea*. *Water, Air, and Soil Pollution*, **227**, 229.
https://doi.org/10.1007/s11270-016-2923-y

[35] Fleck, A.S., Moresco, M.B. and Rhoden, C.R. (2016) Assessing the Genotoxicity of Traffic-Related Air Pollutants by Means of Plant Biomonitoring in Cities of a Brazilian Metropolitan Area Crossed by a Major Highway. *Atmospheric Pollution Research*, **7**, 488-493. https://doi.org/10.1016/j.apr.2015.12.002

[36] El-Baz, F. and Al-Sarawi, M. (2000) Atlas of Kuwait. Kuwait Foundation Advancement Science Press, Kuwait.

[37] Al-Awadhi, J.M. and AlShuaibi, A.A. (2013) Dust Fallout in Kuwait City: Deposition and Characterization. *Science of the Total Environment*, **461-462**, 139-148.
https://doi.org/10.1016/j.scitotenv.2013.03.052

[38] Bangert, M., Nenes, A., Vogel, B., Vogel, H., Barahona, D., Karydis, V.A., Blahak, U., *et al*. (2012) Saharan Dust Event Impacts on Cloud Formation and Radiation over Western Europe. *Atmospheric Chemistry and Physics*, **12**, 4045-4063.
https://doi.org/10.5194/acp-12-4045-2012

[39] Ramos, Y., St-Onge, B., Blanchet, J.P. and Smargiassi, A. (2016) Spatio-Temporal Models to Estimate Daily Concentrations of Fine Particulate Matter in Montreal: Kriging with External Drift and Inverse Distance-Weighted Approaches. *Journal of Exposure Science and Environmental Epidemiology*, **26**, 405-414.
https://doi.org/10.1038/jes.2015.79

[40] Brunekreef, B., Hoek, G., Schouten, L., Bausch-Goldbohm, S., Fischer, P., Armstrong, B., van den Brandt, P., *et al*. (2009) Effects of Long-Term Exposure to Traffic-Related Air Pollution on Respiratory and Cardiovascular Mortality in the Netherlands: The NLCS-AIR Study. *Research Report* (*Health Effects Institute*), No. 139, 5-71.
http://www.ncbi.nlm.nih.gov/pubmed/19554969

[41] Boquete, M.T., Aboal, J.R., Carballeira, A. and Fernández, J.A. (2017) Do Mosses Exist outside of Europe? A Biomonitoring Reflection. *Science of the Total Envi-*

ronment, **593**-**594**, 567-570. https://doi.org/10.1016/j.scitotenv.2017.03.196

[42] Dołęgowska, S. (2017) Measurement Uncertainty from Physical Sample Preparation of Moss Samples: Estimation of Mechanical Cleaning vs. Rinsing. *Ecological Indicators*, **76**, 64-70. https://doi.org/10.1016/j.ecolind.2017.01.004

[43] Bustamante, J., Liñero, O., Arrizabalaga, I., Carrero, J.A., Arana, G. and de Diego, A. (2015) Sample Pretreatment to Differentiate between Bioconcentration and Atmospheric Deposition of Polycyclic Aromatic Hydrocarbons in Mosses. *Chemosphere*, **122**, 295-300. https://doi.org/10.1016/j.chemosphere.2014.11.069

[44] Al-Khashman, O.A., Al-Muhtaseb, A.H. and Ibrahim, K.A. (2011) Date Palm (*Phoenix dactylifera* L.) Leaves as Biomonitors of Atmospheric Metal Pollution in Arid and Semi-Arid Environments. *Environmental Pollution*, **159**, 1635-1640. https://doi.org/10.1016/j.envpol.2011.02.045

[45] Kardel, F., Wuyts, K., Maher, B.A. and Samson, R. (2012) Intra-Urban Spatial Variation of Magnetic Particles: Monitoring via Leaf Saturation Isothermal Remanent Magnetisation (SIRM). *Atmospheric Environment*, **55**, 111-120. https://doi.org/10.1016/j.atmosenv.2012.03.025

[46] Maher, B.A. (2011) The Magnetic Properties of Quaternary Aeolian Dusts and Sediments, and Their Palaeoclimatic Significance. *Aeolian Research*, **3**, 87-144. https://doi.org/10.1016/j.aeolia.2011.01.005

[47] Meena, N.K., Maiti, S. and Shrivastava, A. (2011) Discrimination between Anthropogenic (Pollution) and Lithogenic Magnetic Fraction in Urban Soils (Delhi, India) Using Environmental Magnetism. *Journal of Applied Geophysics*, **73**, 121-129. https://doi.org/10.1016/j.jappgeo.2010.12.003

[48] Al-Awadhi, J.M., Omar, S.A. and Misak, R.F. (2005) Land Degradation Indicators in Kuwait. *Land Degradation and Development*, **16**, 163-176. https://doi.org/10.1002/ldr.666

[49] Engelbrecht, J.P., Moosmüller, H., Pincock, S., Jayanty, R.K.M., Lersch, T. and Casuccio, G. (2016) Technical Note: Mineralogical, Chemical, Morphological, and Optical Interrelationships of Mineral Dust Re-Suspensions. *Atmospheric Chemistry and Physics*, **16**, 10809-10830. https://doi.org/10.5194/acp-16-10809-2016

[50] Fernández, A.J., Ternero, M., Barragán, F.J. and Jiménez, J.C. (2000) An Approach to Characterization of Sources of Urban Airborne Particles through Heavy Metal Speciation. *Chemosphere—Global Change Science*, **2**, 123-136. https://doi.org/10.1016/S1465-9972(00)00002-7

[51] Maity, R., Venkateshwarlu, M., Mondal, S., Kapawar, M.R., Gain, D. and Paul, P. (2020) Magnetic and Microscopic Characterization of Anthropogenically Produced Magnetic Particles: A Proxy for Environmental Pollution. *International Journal of Environmental Science and Technology*, **18**, 1793-1808. https://doi.org/10.1007/s13762-020-02902-x

[52] Turekian, K.K. and Hans Wedepohl, K. (1961) Distribution of the Elements in Some Major Units of the Earth's Crust. *Geological Society of America Bulletin*, **72**, 175-192. https://doi.org/10.1130/0016-7606(1961)72[175:DOTEIS]2.0.CO;2

[53] Van Wittenberghe, S., Alonso, L., Verrelst, J., Hermans, I., Delegido, J., Veroustraete, F., Samson, R., *et al.* (2013) Upward and Downward Solar-Induced Chlorophyll Fluorescence Yield Indices of Four Tree Species as Indicators of Traffic Pollution in Valencia. *Environmental Pollution*, **173**, 29-37. https://doi.org/10.1016/j.envpol.2012.10.003

[54] Declercq, Y., Samson, R., Van De Vijver, E., De Grave, J., Tack, F.M.G. and De Smedt, P. (2020) A Multi-Proxy Magnetic Approach for Monitoring Large-Scale

Airborne Pollution Impact. *Science of the Total Environment*, **743**, Article ID: 140718. https://doi.org/10.1016/j.scitotenv.2020.140718

[55] Xia, D.S., Jia, J., Wei, H.T., Liu, X.B., Ma, J.Y., Wang, X.M. and Chen, F.H. (2012) Magnetic Properties of Surface Soils in the Chinese Loess Plateau and the Adjacent Gobi Areas, and Their Implication for Climatic Studies. *Journal of Arid Environments*, **78**, 73-79. https://doi.org/10.1016/j.jaridenv.2011.10.012

[56] Dekkers, M.J. (2007) Magnetic Proxy Parameters.

[57] Lu, S.G. and Bai, S.Q. (2006) Study on the Correlation of Magnetic Properties and Heavy Metals Content in Urban Soils of Hangzhou City, China. *Journal of Applied Geophysics*, **60**, 1-12. https://doi.org/10.1016/j.jappgeo.2005.11.002

[58] Lu, S.G. and Bai, S.Q. (2008) Magnetic Characterization and Magnetic Mineralogy of the Hangzhou Urban Soils and Its Environmental Implications. *Acta Geophysica Sinica*, **51**, 762-769. https://doi.org/10.1002/cjg2.1245

[59] Wang, G., Oldfield, F., Xia, D., Chen, F., Liu, X. and Zhang, W. (2012) Magnetic Properties and Correlation with Heavy Metals in Urban Street Dust: A Case Study from the City of Lanzhou, China. *Atmospheric Environment*, **46**, 289-298. https://doi.org/10.1016/j.atmosenv.2011.09.059

[60] Watkins, S.J. and Maher, B.A. (2003) Magnetic Characterisation of Present-Day Deep-Sea Sediments and Sources in the North Atlantic. *Earth and Planetary Science Letters*, **214**, 379-394. https://doi.org/10.1016/S0012-821X(03)00422-9

[61] Qian, P., Zheng, X., Zhou, L., Jiang, Q., Zhang, G. and Yang, J. (2011) Magnetic Properties as Indicator of Heavy Metal Contaminations in Roadside Soil and Dust along G312 Highways. *Procedia Environmental Sciences*, **10**, 1370-1375. https://doi.org/10.1016/j.proenv.2011.09.219

[62] Roberts, A.P., Zhao, X., Heslop, D., Abrajevitch, A., Chen, Y.H., Hu, P., Pillans, B.J., *et al.* (2020) Hematite (α-Fe$_2$O$_3$) Quantification in Sedimentary Magnetism: Limitations of Existing Proxies and Ways Forward. *Geoscience Letters*, **7**, Article No. 8. https://doi.org/10.1186/s40562-020-00157-5

[63] Wang, B., Xia, D., Yu, Y., Chen, H. and Jia, J. (2018) Source Apportionment of Soil-Contamination in Baotou City (North China) Based on a Combined Magnetic and Geochemical Approach. *Science of the Total Environment*, **642**, 95-104. https://doi.org/10.1016/j.scitotenv.2018.06.050

[64] Nie, J., Song, Y., King, J. W., Fang, X. and Heil, C. (2010) HIRM Variations in the Chinese Red-Clay Sequence: Insights into Pedogenesis in the Dust Source Area. *Journal of Asian Earth Sciences*, **38**, 96-104. https://doi.org/10.1016/j.jseaes.2009.11.002

[65] Frank, U. and Nowaczyk, N.R. (2008) Mineral Magnetic Properties of Artificial Samples Systematically Mixed from Haematite and Magnetite. *Geophysical Journal International*, **175**, 449-461. https://doi.org/10.1111/j.1365-246X.2008.03821.x

[66] Mitchell, R., Maher, B.A. and Kinnersley, R. (2010) Rates of Particulate Pollution Deposition onto Leaf Surfaces: Temporal and Inter-Species Magnetic Analyses. *Environmental Pollution*, **158**, 1472-1478. https://doi.org/10.1016/j.envpol.2009.12.029

[67] Bayraktar, H., Turalioğlu, F.S. and Tuncel, G. (2010) Average Mass Concentrations of TSP, PM$_{10}$ and PM$_{2.5}$ in Erzurum Urban Atmosphere, Turkey. *Stochastic Environmental Research and Risk Assessment*, **24**, 57-65. https://doi.org/10.1007/s00477-008-0299-2

[68] Rezazadeh, M., Irannejad, P. and Shao, Y. (2013) Climatology of the Middle East dust Events. *Aeolian Research*, **10**, 103-109.

https://doi.org/10.1016/j.aeolia.2013.04.001

[69] Hofman, J., Stokkaer, I., Snauwaert, L. and Samson, R. (2013) Spatial Distribution Assessment of Particulate Matter in an Urban Street Canyon Using Biomagnetic Leaf Monitoring of Tree Crown Deposited Particles. *Environmental Pollution*, **183**, 123-132. https://doi.org/10.1016/j.envpol.2012.09.015

[70] Zhang, C., Huang, B., Piper, J.D.A. and Luo, R. (2008) Biomonitoring of Atmospheric Particulate Matter Using Magnetic Properties of *Salix matsudana* Tree Ring Cores. *Science of the Total Environment*, **393**, 177-190. https://doi.org/10.1016/j.scitotenv.2007.12.032

[71] Kermani, M., Jafari, A., Gholami, M., Fanaei, F. and Arfaeinia, H. (2020) Association between Meteorological Parameter and $PM_{2.5}$ Concentration in Karaj, Iran. *International Journal of Environmental Health Engineering*, **9**, 1-6.

[72] Shukla, K., Kumar, P., Mann, G.S. and Khare, M. (2020) Mapping Spatial Distribution of Particulate Matter Using Kriging and Inverse Distance Weighting at Supersites of Megacity Delhi. *Sustainable Cities and Society*, **54**, Article ID: 101997. https://doi.org/10.1016/j.scs.2019.101997

[73] Al-Nassar, W., Alhajraf, S., Al-Enizi, A. and Al-Awadhi, L. (2005) Potential Wind Power Generation in the State of Kuwait. *Renewable Energy*, **30**, 2149-2161. https://doi.org/10.1016/j.renene.2005.01.002

[74] Strzyszcz, Z. (1995) Gehalt an Ferromagnetika in den von der Immision der Zement-industrie in der Wojewodschaft Opole beeinflussten Böden (Contents of Ferromagnetics in Soils of Opole Region Contaminated by Cement-Industry Imissions). *Mitteilungen der DBG—Deutsche Bodenkundliche Gesellschaft*, **76**, 1477-1480.

[75] Petrovský, E., Kapička, A., Jordanova, N., Knab, M. and Hoffmann, V. (2000) Low-Field Magnetic Susceptibility: A Proxy Method of Estimating Increased Pollution of Different Environmental Systems. *Environmental Geology*, **39**, 312-318. https://doi.org/10.1007/s002540050010

[76] Rai, P.K., Chutia, B.M. and Patil, S.K. (2014) Monitoring of Spatial Variations of Particulate Matter (PM) Pollution through Bio-Magnetic Aspects of Roadside Plant Leaves in an Indo-Burma Hot Spot Region. *Urban Forestry and Urban Greening*, **13**, 761-770. https://doi.org/10.1016/j.ufug.2014.05.010

[77] Huang, H., Ooka, R., Chen, H., Kato, S., Takahashi, T. and Watanabe, T. (2008) CFD Analysis on Traffic-Induced Air Pollutant Dispersion under Non-Isothermal Condition in a Complex Urban Area in Winter. *Journal of Wind Engineering and Industrial Aerodynamics*, **96**, 1774-1788. https://doi.org/10.1016/j.jweia.2008.02.010

[78] Engelbrecht, J.P., McDonald, E.V., Gillies, J.A., Jayanty, R.K.M., Casuccio, G. and Gertler, A.W. (2009) Characterizing Mineral Dusts and Other Aerosols from the Middle East—Part 2: Grab Samples and Re-Suspensions. *Inhalation Toxicology*, **21**, 327-336. https://doi.org/10.1080/08958370802464299

[79] Di Sabatino, S., Buccolieri, R., Pulvirenti, B. and Britter, R. (2007) Simulations of Pollutant Dispersion within Idealised Urban-Type Geometries with CFD and Integral Models. *Atmospheric Environment*, **41**, 8316-8329. https://doi.org/10.1016/j.atmosenv.2007.06.052

[80] Shilton, V.F., Booth, C.A., Smith, J.P., Giess, P., Mitchell, D.J. and Williams, C.D. (2005) Magnetic Properties of Urban Street Dust and Their Relationship with Organic Matter Content in the West Midlands, UK. *Atmospheric Environment*, **39**, 3651-3659. https://doi.org/10.1016/j.atmosenv.2005.03.005